



1

UNCLASS

SECURITY CLASSIFICATION OF THIS PAGE (When Data Entered)

AD A116738

REPORT DOCUMENTATION PAGE		READ INSTRUCTIONS BEFORE COMPLETING FORM
1. REPORT NUMBER AFIT/NR/82-6T	2. GOVT ACCESSION NO. AD-A116738	3. RECIPIENT'S CATALOG NUMBER
4. TITLE (and Subtitle) Geophysical Investigation of the Raton Basin		5. TYPE OF REPORT & PERIOD COVERED THESIS/DISSERTATION
		6. PERFORMING ORG. REPORT NUMBER
7. AUTHOR(s) Richard Stephen Cheney		8. CONTRACT OR GRANT NUMBER(s)
9. PERFORMING ORGANIZATION NAME AND ADDRESS AFIT STUDENT AT: Texas Tech University		10. PROGRAM ELEMENT, PROJECT, TASK AREA & WORK UNIT NUMBERS
11. CONTROLLING OFFICE NAME AND ADDRESS AFIT/NR WPAFB OH 45433		12. REPORT DATE May 1982
		13. NUMBER OF PAGES 78
14. MONITORING AGENCY NAME & ADDRESS (if different from Controlling Office)		15. SECURITY CLASS. (of this report) UNCLASS
		15a. DECLASSIFICATION/DOWNGRADING SCHEDULE
16. DISTRIBUTION STATEMENT (of this Report) APPROVED FOR PUBLIC RELEASE; DISTRIBUTION UNLIMITED		
17. DISTRIBUTION STATEMENT (of the abstract entered in Block 20, if different from Report)  LYNN E. WOLAVER Dean for Research and Professional Development AR FOR THE INSTITUTE OF TECHNOLOGY (ATC) WRIGHT-PATTERSON AFB, OH 45433		
18. SUPPLEMENTARY NOTES APPROVED FOR PUBLIC RELEASE: IAW AFR 190/17 22 JUN 1982		
19. KEY WORDS (Continue on reverse side if necessary and identify by block number)		
20. ABSTRACT (Continue on reverse side if necessary and identify by block number) ATTACHED		

DTIC FILE COPY

82 07 07 058

DTIC  
ELECT  
JUL 09 1982  
S E

DD FORM 1473 EDITION OF 1 NOV 68 IS OBSOLETE

UNCLASS

SECURITY CLASSIFICATION OF THIS PAGE (When Data Entered)

"Original contains color plates: All DTIC reproductions will be in black and white"

THESIS ABSTRACT

Name: Richard S. Cheney

Title: Geophysical Investigation of the Raton Basin

Rank: Captain, USAF, 1982

Degree: Master of Science in Geosciences, Texas Tech University

✓  
This thesis correlates gravity, magnetic, and seismic data for the Raton Basin of Colorado and New Mexico. The gravity data suggest that the study area, and the region around it, is in isostatic equilibrium. The free air anomaly in the southern portion of the study area suggests lack of local compensation due to Quaternary volcanic rock. The volcanic rock thickness, calculated from the free air gravity data, is 180 m. The gravity data indicated a crustal thickness of about 45 km, and the crust thinned from west to east.

A basement relief map was constructed from the Bouguer gravity data. Computer techniques were developed to calculate the depth to the basement surface and to plot a contour map of that surface. The Raton Basin magnetic map defined the same surface found on the basement relief map since the overlying sedimentary rocks have no magnetism; therefore, any magnetism present is caused by the basement rock.

A seismic survey near Capulin Mountain detected a high level of micro-seismicity that may be caused by adjustment along faults or dormant volcanic activity.

↑  
P-1  
"Original contains color plates: All DTIC reproductions will be in black and white"

82-6T

GEOPHYSICAL INVESTIGATION OF THE RATON BASIN

by

RICHARD STEPHEN CHENEY, A.B., M.A.

A THESIS

IN

GEOSCIENCE

Submitted to the Graduate Faculty  
of Texas Tech University in  
Partial Fulfillment of  
the Requirements for  
the Degree of

MASTER OF SCIENCE

Approved

*A. H. Shubert*  
Chairman of the Committee

*S. E. Cobell*

Accepted

*John Jones*  
Dean of the Graduate School

Accession For	
NTIS GRA&I	<input checked="" type="checkbox"/>
DTIC TAB	<input type="checkbox"/>
Unannounced	<input type="checkbox"/>
Justification	
By _____	
Distribution/	
Availability Codes	
Dist	Avail and/or Special
<b>A</b>	

May, 1982



#### ACKNOWLEDGEMENTS

The author recognizes the criticisms and advice of Professors S.E. Cebull, J.R. Giardino, and D.H. Shurbet in the preparation of this thesis. Technical advice in computer techniques and graphics was offered by J.R. Giardino and C.W. Baugh of Texas Tech University. The color reproduction of cartographic plates was arranged by Doctors L. Decker, and R. Ballew of the Defense Mapping Agency, St. Louis Air Force Station, Missouri. Mr. R. Wolfe of Teledyne Geotech Corporation, Garland, Texas, provided technical support in the operation of seismic equipment provided by his company under Air Force contract F08606-80-C-0014. Mrs. J.J. Wolff and Doctors D. Cash and K. Olsen of the Los Alamos Laboratory, New Mexico, supported, encouraged and helped evaluate the seismic data of this thesis. Finally, the author extends his sincere appreciation to his wife, Linda, whose moral support and inspiration made this thesis possible.

Partial funding for the preparation of this thesis was provided by the United States Air Force Institute of Technology under the following agreements: ESA - F33600-75-A; TA - 330 (4 MAR 81), and TD - 37 (6 JUL 81).

## CONTENTS

	Page
ACKNOWLEDGMENTS . . . . .	ii
LIST OF TABLES . . . . .	v
LIST OF ILLUSTRATIONS . . . . .	vi
CHAPTER	
I. INTRODUCTION . . . . .	1
General Statement . . . . .	1
Purpose of the Investigation . . . . .	2
General Geology of the Basin . . . . .	3
II. DATA COLLECTION AND REDUCTION . . . . .	12
General Statement . . . . .	12
Elevation Control . . . . .	12
Magnetic Data Measurement and Reduction . . . . .	13
Gravity Data Measurement and Reduction . . . . .	13
Seismic Data . . . . .	14
Computer Processing Techniques . . . . .	14
III. PRESENTATION AND INTERPRETATION OF THE GRAVITY, MAGNETIC, AND SEISMIC DATA . . . . .	17
Free Air Gravity Data . . . . .	17
Bouguer Gravity Data . . . . .	25
Raton Basin Basement Structure Map . . . . .	32
Raton Basin Magnetic Map . . . . .	40

Capulin Local Seismic Study . . . . .	43
IV. CONCLUSIONS . . . . .	50
REFERENCES CITED . . . . .	51
APPENDIX A . . . . .	54
APPENDIX B . . . . .	70
APPENDIX C . . . . .	73

LIST OF TABLES

Table	Page
1. Theoretical and actual gravity anomalies in the study area . . . . .	31
2. Recorded earthquake activity in the study area of New Mexico 1900-1981 . . . . .	46

## LIST OF ILLUSTRATIONS

Figure	Page
1. Geologic structures defining the Raton Basin of New Mexico and Colorado . . . . .	2
2. Location of the study area and limits to each survey in this report . . . . .	4
3. Columnar section of the Las Vegas and Raton Basins . . .	6
4. Regional free air gravity map using NOAA gravity data . .	18
5. Regional free air anomaly map of the study area . . . . .	19
6. Graphic representation of the algebraic averages of the NOAA gravity and elevation data divided into one degree latitude and longitude blocks . . . . .	20
7. Regional topographic map of the study area . . . . .	23
8. Capulin free air gravity map . . . . .	24
9. Plot of the averaged NOAA elevation data vs. the averaged NOAA Bouguer gravity data . . . . .	26
10. Regional Bouguer gravity map using NOAA gravity data . .	27
11. Regional Bouguer anomaly map of the study area . . . . .	28
12. Capulin Bouguer gravity map . . . . .	33
13. Basement structure profile derived from NOAA Bouguer gravity data along 37°N, 104°-105°W . . . . .	37
14. Raton Basin magnetic map . . . . .	41
15. Capulin magnetic map . . . . .	44
16. Geographic location of seismic events strong enough to be felt by local population in northeast New Mexico from 1900 to 1980. . . . .	45

Figure	Page
17. Bar graph representation of the frequency of seismic events in Table 2 in five year increments . . . . .	47
18. Seismograms from the Capulin seismic survey . . . . .	49

Plate	Page
1. Geology and structure of the Raton Basin of N.M. and Colo. . . . .	76
2. Basement structure map of the Raton Basin of N.M. and Colo. . . . .	77
3. Magnetic Map of the Raton Basin of N.M. and Colo. . . . .	78

## CHAPTER I

### INTRODUCTION

#### General Statement

The Raton Basin of New Mexico and Colorado ( $35^{\circ}$ - $38^{\circ}$ N;  $104^{\circ}$ - $105.5^{\circ}$ W) is a structural depression which is defined by the Sangre de Cristo Uplift on the West, the Wet Mountains Uplift to the north, the Apishipa Arch on the northeast, and the Sierra Grande Arch on the southeast (figure 1). Today the Raton Basin is outlined by topographic relief caused by the caprock "effect" of the Trinidad Sandstone. The importance of the outlining "effect" of the Trinidad Sandstone is illustrated by both Baltz (1965) and Brill (1952) who draw the eastern boundary of the Raton Basin at the outcrop of Trinidad Sandstone, rather than along the axes of the Apishipa and Sierra Grande Arches.

Extending 175 miles long and a maximum of 65 miles wide, the Raton Basin is divided by the Cimarron Arch into the northern Raton Basin and the Las Vegas Basin on the south. The deepest depression within the Basin is located near the Sangre de Cristo Uplift. Rocks on the west limb of the Basin dip vertically, whereas rocks on the east limb dip one to five degrees (Wanek, 1963). In this thesis, the entire Raton Basin will be referred to as the Basin, while the northern portion will be called the Raton Basin, and the southern portion referred to as the Las Vegas Basin.

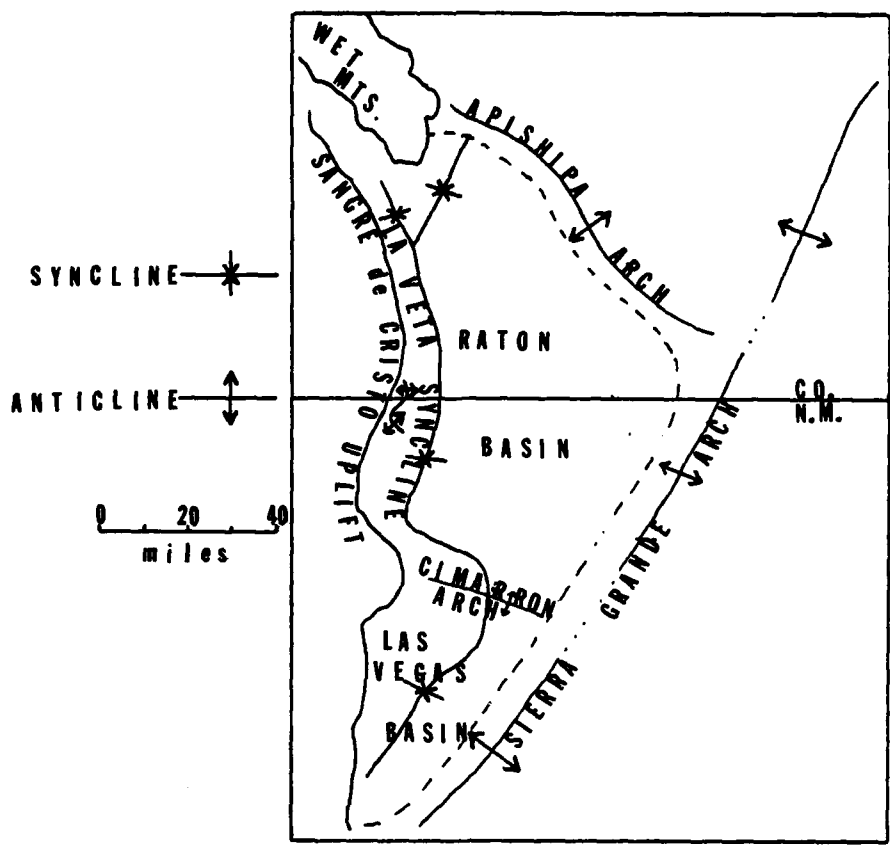


Figure 1. Geologic structures defining the Raton Basin of New Mexico and Colorado.

Purpose of the Investigation

Knowledge of the Basin is incomplete, and correlation of geophysical and geologic data has not been previously published. Therefore, in order to fill this void in the literature this thesis will undertake the following objectives: 1) Obtain and interpret both Free Air and Bouguer Gravity maps; 2) Obtain and interpret a vertical component magnetic map; 3) Obtain vertical, short-period seismic records for the Capulin area in an effort to determine the natural seismic activity; 4) Compare

geophysical data with the geologic structure, and 5) Determine whether economic potential in the Basin can be inferred from geophysical data. The study being reported here includes gravity, magnetic, and seismic surveys of portions of the Basin, including the Sierra Grande Arch and adjacent High Plains (figure 2).

#### General Geology of the Basin

The first of the two orogenies that have affected the Basin occurred during Pennsylvanian and Permian time (Baltz, 1965), and was responsible for detritus filling the Central Colorado Basin (located in the northern portion of the Raton Basin). The detrital material was derived from both west (San Luis Uplift) and east (the ancestral Wet Mountains Uplift) of the Basin. Contemporaneously, the Rowe-Mora Basin, which was in the general vicinity of the present Las Vegas Basin, also formed. This Basin was defined by the San Luis Uplift to the west, the Sierra Grande Uplift to the east, the Cimarron Arch on the north, and was linked by a low saddle to the Tucumcari Basin to the south. The Colorado and Rowe-Mora Basins filled with sediments which were derived from the ancestral Rockies and deposited in a marine transgressive environment of Pennsylvanian age. The resulting strata show a laterally complex composition reflecting the mixed terrestrial-marine origin. These strata are thickest in the regime of the Sangre de Cristo Mountains. Large accumulations of sandstone and limestone occur in the southern portion of the Rowe-Mora Basin, but shale deposits, which are dominated by thick grey to black strata, predominate to the north. In fact, this shale which

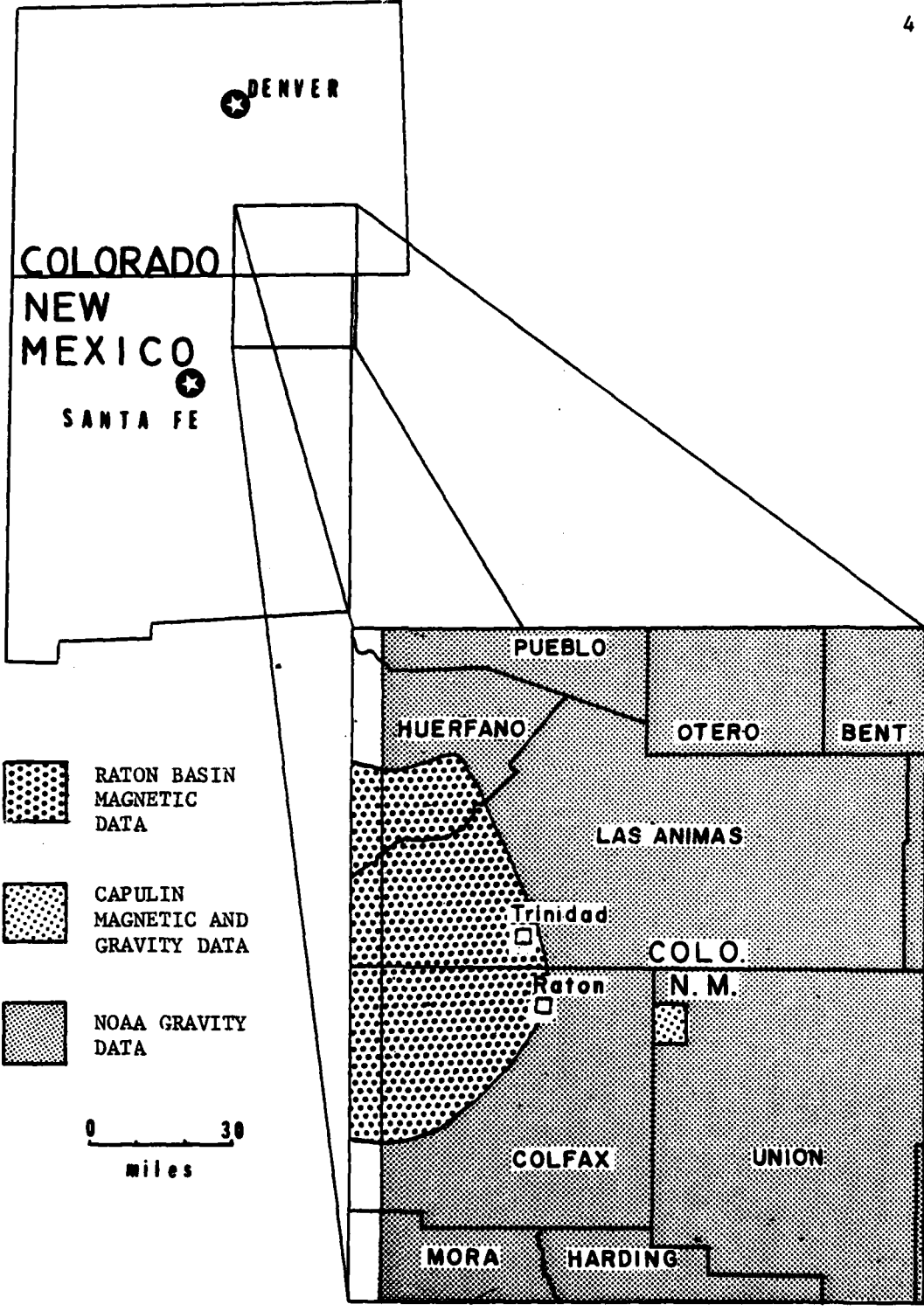


Figure 2. Location of the study area and limits to each survey in this report.

characterizes the northern part of the ancient Central Colorado Basin is a minimum of 9,500 feet thick (Brill, 1952). On the margins of the ancient basins, shale deposits thin towards the San Luis, Sierra Grande, and Wet Mountains Uplifts.

The depositional history of the strata in the Basin is complex as is the correlation between contemporaneous formations in the Las Vegas and Raton Basins (figure 3). Strata which were deposited in the Permian era are dominated by marine shales and clastic rocks. Triassic strata are composed primarily of terrestrial clastic rocks but are, however, sparsely represented in the area. Today the Las Vegas Basin area is covered partially by Quaternary volcanic rocks. Discussion of the depositional and orogenic history is limited to the area of the present Basin and is based on rock outcrops and the known geologic structure (plate 1).

The oldest rocks identified in the Basin are marine sandstones and limestones of the Devonian Espiritu Santo Formation (Baltz, 1965) in the Las Vegas Basin and the Devonian Chaffee Formation (Johnson, 1969) in the Raton Basin. Limestone breccia of the Mississippian Tererro Formation rests unconformably on the Espiritu Santo Formation in the Las Vegas Basin. The Tererro Formation is missing in the Raton Basin.

The Pennsylvanian Magdalena Group is composed of sandstone and grey shale of the Sandia Formation and limestone of the overlying Madera Formation. The Sandia Formation in the Las Vegas Basin, which consists of over 1,000 feet of sedimentary rock, is correlative with the Deer Creek Formation and the lower part of the Minturn Formation of the Raton Basin.



The Madera limestone ranges from 1,000 to 3,000 feet in thickness in the Las Vegas Basin; it grades laterally northward into the Minturn Formation, which has a thickness of 5,500 feet. These units thin to the west and east of the Basin in the general direction of the San Luis and Sierra Grande Uplifts.

The Upper Pennsylvanian/Permian Sangre de Cristo Formation is approximately 3,500 feet thick in the Las Vegas Basin and greater than 9,500 feet thick in the Raton Basin (figure 3).

At the end of the Permian time a sea filled the Rowe-Mora Basin, and deposition of siltstone and shale of the Yeso Formation began. Located above the Yeso Formation is the Glorieta Sandstone and San Andreas Limestone, respectively. Overlying the San Andreas Limestone is the Bernal Formation which is composed of limestone, siltstone, shale, and sandstone. These three formations have a combined, maximum thickness of 1,075 feet (figure 3).

The Late Triassic Dockum Group lies conformably on Permian strata. In the Las Vegas Basin the Group is composed of both the Santa Rosa Sandstone and the overlying Chinle Formation shales. North of the Cimarron Arch the Dockum Group is correlative to the Johnson Gap Formation, which is composed of limestone conglomerate, limestone, siltstone, shale, and sandstone (Baltz, 1965). The Dockum Group is approximately 1,100 feet thick in the Las Vegas Basin and less than 700 feet thick in the Raton Basin.

By Early Cretaceous time the region was part of the Rocky Mountain geosyncline. The Laramide Orogeny, the second orogeny to affect the

area, continued from Cretaceous time through Oligocene time and produced the present Las Vegas and Raton Basins and other associated structures. At the beginning of the orogeny, the San Luis Uplift was still a positive area. By Eocene time the present Raton Basin was defined by the marked uplift of the Sangre de Cristo region and the gentle uplift of the Apishipa-Sierra Grande Arches. The Sangre de Cristo Uplift merged with the San Luis Uplift prior to the formation of the Rio Grande rift. When the Rio Grande rift formed in Miocene/Pliocene time, the San Luis positive area was downfaulted into the rift graben.

The Early Cretaceous Purgatoire Formation is composed of both conglomeratic sandstone and sandstone. The Dakota Sandstone overlies the Purgatoire Formation and is composed of interbedded, buff sandstone and shale. Together, these two formations are up to 650 feet thick, and today they form the primary groundwater aquifer in the Basin. Estimates place the volume of water stored in the Dakota Sandstone at 55 million acre-feet in New Mexico (Griggs, 1948); twice the above volume is estimated for the Basin.

The Graneros Shale, Greenhorn Limestone, and Carlile Shale are Late Cretaceous in age and vary in thickness from 385 feet to 700 feet (Baltz, 1965). The Upper Cretaceous Niobrara Formation is composed of less than 100 feet of shale and sandstone and rests conformably on the Carlile Shale.

Located on top of the Niobrara Formation is the Upper Cretaceous Pierre Shale, which is up to 2,300 feet thick in the Raton Basin but is absent in the Las Vegas Basin. The formation is composed of shale,

thin beds of limestone, and sandstone. Above the Pierre Shale are the Upper Cretaceous Trinidad Sandstone and Vermejo Formation, which are undifferentiated on some geological maps (Bachman and Dane, 1962). The Trinidad Sandstone is composed of arkosic sandstone with thin interbedded shale; it intertongues with the shale, coal, and arkosic sandstone of the Vermejo Formation. The thickness of the two formations varies from 250 feet to 850 feet. The Vermejo Formation is the main source of coal in the Basin, producing high volatile C bituminous coal of coking quality (Wanek, 1963). In the areas of extensive intrusive rocks, much of the coal was destroyed by contact metamorphism (Jurie and Gerhard, 1969).

The Raton Formation is Late Cretaceous to Early Tertiary in age and overlies the Vermejo Formation. It has a maximum thickness of 1,700 feet and is composed of arkosic sandstone, shale, and coal. The Poison Canyon Formation of Paleocene age lies unconformably on the Raton Formation. It consists of as much as 2,500 feet of arkosic sandstone, conglomerate, and thin shale. The youngest significant formation in the Basin is the Cuchara Formation, which is exposed around Spanish Peaks. It is Eocene in age and is composed of conglomeratic sandstone and interbedded shale.

During the latter stages of the Laramide Orogeny numerous intrusive rocks penetrated the sedimentary rocks. Dike swarms, sills, stocks and laccoliths dating from Eocene/Oligocene time are found throughout the Basin. However, the greatest concentration is found in the Spanish Peaks intrusive area. Many small anticlines are attributed to the intrusive

upwelling. Emplacement of many of the dikes, which are silicic to ultra basic in composition, appears to have been fault controlled (Wanek, 1963).

Volcanic activity was concentrated near the Sierra Grande Arch. Baldwin and Muehlberger (1959) identified three sequences of volcanic flows, dating from Miocene to Recent, that they called Raton, Clayton, and Capulin, respectively. Both the Raton and Capulin sequences are composed of basalts, and the Clayton sequence has a varied composition which ranges from extremely alkalic to subsilicic. Geochemical analysis of the volcanic rock suggests the magma originated in the upper mantle (Jones et al., 1976). Stormer (1972) suggests eastward migration of the vulcanism across the Rio Grande rift, from the San Juan volcanic field to the Sierra Grande volcanic field, occurred. Sanford et al., (1981) also suggest that the Sierra Grande vulcanism might be an eastern extension of the Jemez Lineation of western New Mexico. Further, Hamilton and Pakiser (1965) indicate that the Rio Grande rift is limited to the upper crust. Thus, the mantle may be the magma source in vulcanism on both sides of the rift.

It has been suggested (Edwards et al., 1978) that anomalously high heat flows may be caused by igneous activity within the Basin. Typical heat flow values for the Great Plains average 1.5 HFU (1 HFU =  $1\mu\text{cal}/\text{cm}^2$  sec), but values as high as 4.7 HFU are found in the Basin. Suppe et al., (1975) proposed a hot spot trace from eastern Arizona to a location near Raton, New Mexico. Reiter et al., (1979) theorized that a thermal anomaly formerly existed east of the Southern Rocky Mountains and is now

centered near the Sierra Grande Arch. They noted that radioactivity of the sedimentary rocks within the Basin can account for only ten percent of the observed increased heat flow; the remainder is unexplained.

In summary, the total thickness of sedimentary fill in the Basin is about 17,000 feet. The Basin sediments date from Middle Paleozoic time and have been affected by two orogenies. These sedimentary rocks have economic importance, and mining activities in the Raton Basin have produced coal and graphite in commercial quantities. Cretaceous rocks are also known to have both oil and gas in small quantities. Currently, there is one commercial oil well in Huerfano County, Colorado, at the northern end of the Basin, and a gas field near the Basin in eastern Las Animas County, Colorado. A basement structure map will be developed in Chapter III using the densities of the sediments described above, and the gravity data that will be introduced in Chapter II.

## CHAPTER II

### DATA COLLECTION AND REDUCTION

#### General Statement

A portion of the gravity data used in this study were obtained from the National Oceanic and Atmospheric Administration (NOAA), Washington, D.C. The gravity and magnetic measurements in the vicinity of Capulin National Monument, New Mexico and the magnetic measurements in the Raton Basin were made by the author during 1981. Each gravity station in the vicinity of Capulin National Monument was also a magnetic station. In order to provide a detailed analysis of the Basin, additional magnetic stations were spaced midway between the gravity stations. NOAA station density is 0.06341 station per square mile; Capulin gravity station density is 1.333 stations per square mile; and Raton Basin magnetic station density is 0.0650 station per square mile.

#### Elevation Control

U.S. Geological Survey fifteen minute quadrangle maps were used to determine elevations for stations near Capulin. Such elevation data were supplemented with a preliminary Bureau of Land Management map of Capulin National Monument. Spot elevations on the maps at road intersections and benchmarks were used wherever possible. Elevation accuracy is within five feet, corresponding to  $\pm 0.35$  mgal accuracy in gravity measurement. Elevation effects were insignificant in the reduction of

the magnetic data.

#### Magnetic Data Measurement and Reduction

The Capulin magnetic data were collected using an E.J. Sharpe PMF-3 flux gate magnetometer (50 and 100 gammas per division). Station number one (figure 14) was arbitrarily chosen by the author as the datum for the survey. Station reoccupation resulted in a minimum of three datum measurements each day and a minimum of two cross correlations on stations occupied on previous days. Diurnal correction graphs were computed daily, and were used to adjust all measurements.

The Raton Basin magnetic data were collected using an Askania vertical Torsion magnetometer (2.433 gammas/degree-scale division). Field procedures for the Raton magnetic survey were the same as those employed in the Capulin magnetic survey. Normal field corrections were computed from  $36^{\circ}30'N$ ,  $105^{\circ}15'W$  using the Regional Vertical Intensity Map 1965. Latitude correction was 909.09 gammas per degree latitude (12.98 gammas per mile); longitude correction was 434.80 gammas per degree longitude (7.9 gammas per mile).

#### Gravity Data Measurement and Reduction

Datum for gravity data acquired from NOAA is sea level. The density used in Bouguer anomaly calculations was 2.67 g/cc. Gravity data acquired near Capulin National Monument were collected using a North American gravimeter (0.107 mgal per division). Station number one was

selected to coincide with a NOAA station in the survey area and was used as the datum for the Capulin survey. This procedure allowed comparison of the Capulin data to the NOAA data. Latitude corrections were made from 36°48'18"N at a rate of 1.25 mgal per mile.

#### Seismic Data

A short period vertical Geotech 18300 seismometer with a free period of one second was buried approximately two feet in depth at the Visitor's Center, Capulin National Monument, from 16 July 1981, to 23 September 1981. During this period, 51 daily seismograms containing 1,122 hours of data were recorded by a Sprengnether VR-50 recorder-amplifier. Damping was increased after 14 August 1981 from normal internal resistance to 2,200 ohms resistance across the input terminals of the amplifier. Filters were not used.

Each seismogram contains twenty-four hours of data with the minute marks spaced sixty millimeters apart. The ink trace was approximately 1.0 mm thick and makes it impossible to resolve frequencies higher than one Hertz. Estimated amplification from artificial inputs is between 25,000 to 50,000.

#### Computer Processing Techniques

Modified computer programs from Davis (1973) and new programs written by the author for this study were employed to process both magnetic and gravity data on an IBM 360 computer housed at Texas Tech University. The machine processing helped to verify manual calculations and also to derive mathematical models that would have been impossible to obtain by

other means.

All data were systematically processed in the same manner. First, the corrected data were filtered by a uniform matrix of either 1,600 or 2,400 elements. The matrix value of each element was obtained by calculating the algebraic average of the six nearest data values. Development of the matrix by interpolation over six data values for each element results in the minimum and the maximum values in the completed matrix to be less than the minimum and the maximum values in the input data. Less than six data values in the interpolation increased the minimum-maximum range in the matrix; however, the areal extent of the maximum and the minimum features would have appeared exaggerated in the final map. This causes mountain peaks to appear as elevated buttes or mesas. The use of more than six data values in interpolation resulted in excessively reducing the minimum-maximum range in the matrix.

Statistical Analysis System's SAS/GRAPH (Reinhardt, 1981) was used to produce the computer maps from the interpolated matrix. These maps were contoured on a strict mathematical ratio by the computer; therefore, the technique can be used advantageously to compare different data sets (gravity and magnetic) produced at the same scale and in the same geographic area. In order to compare the different mapping techniques, both computer plotted and hand drawn maps using the same data sets have been included in this report.

The computer also was used to compare the computer contoured map of the data contained in matrix form to a surface defined by a polynomial of order  $n$ . A polynomial of order 0 represents a dipping plane, and polynomials of very high order very accurately represent the data in

matrix form. A second order polynomial was found to accurately represent the steep gravity dip under the Sangre de Cristo Mountains and the shallow gravity dip of the Great Plains. The residual gravity (Smith, 1970; Dobrin, 1976), or difference, of the second order polynomial from the matrix gravity data was used to construct the basement structure map described in Chapter III.

## CHAPTER III

### PRESENTATION AND INTERPRETATION OF THE GRAVITY, MAGNETIC, AND SEISMIC DATA

#### Free Air Gravity Data

The NOAA free air gravity data have been tabulated and included in Appendix A. The gravity data acquired in the Capulin area as part of this study, which will be discussed as an addition to the NOAA data, have been tabulated and included in Appendix B.

The NOAA free air gravity anomaly data are shown, for comparison, in hand drawn (figure 4) and computer plotted (figure 5) formats. The algebraic averages for the station elevation, free air anomaly, and Bouguer anomaly in each one degree block in the study area are shown in figure 6. The free air anomalies for the northern two blocks of the study area are nearly zero and suggest isostatic equilibrium for this area. However, the free air anomalies are significantly positive in the southern two blocks of the study area and could indicate lack of local isostatic adjustment in these areas. The question of regional isostatic equilibrium is, therefore, raised.

Perfect isostatic adjustment assumes that any near surface positive mass has an equal amount of negative mass below the compensation level within the Earth, and in the simple case, such a mass distribution would cause near zero free air gravity anomalies. However, in elevated terrain, as in the study area, the gravitational effect upon a surface

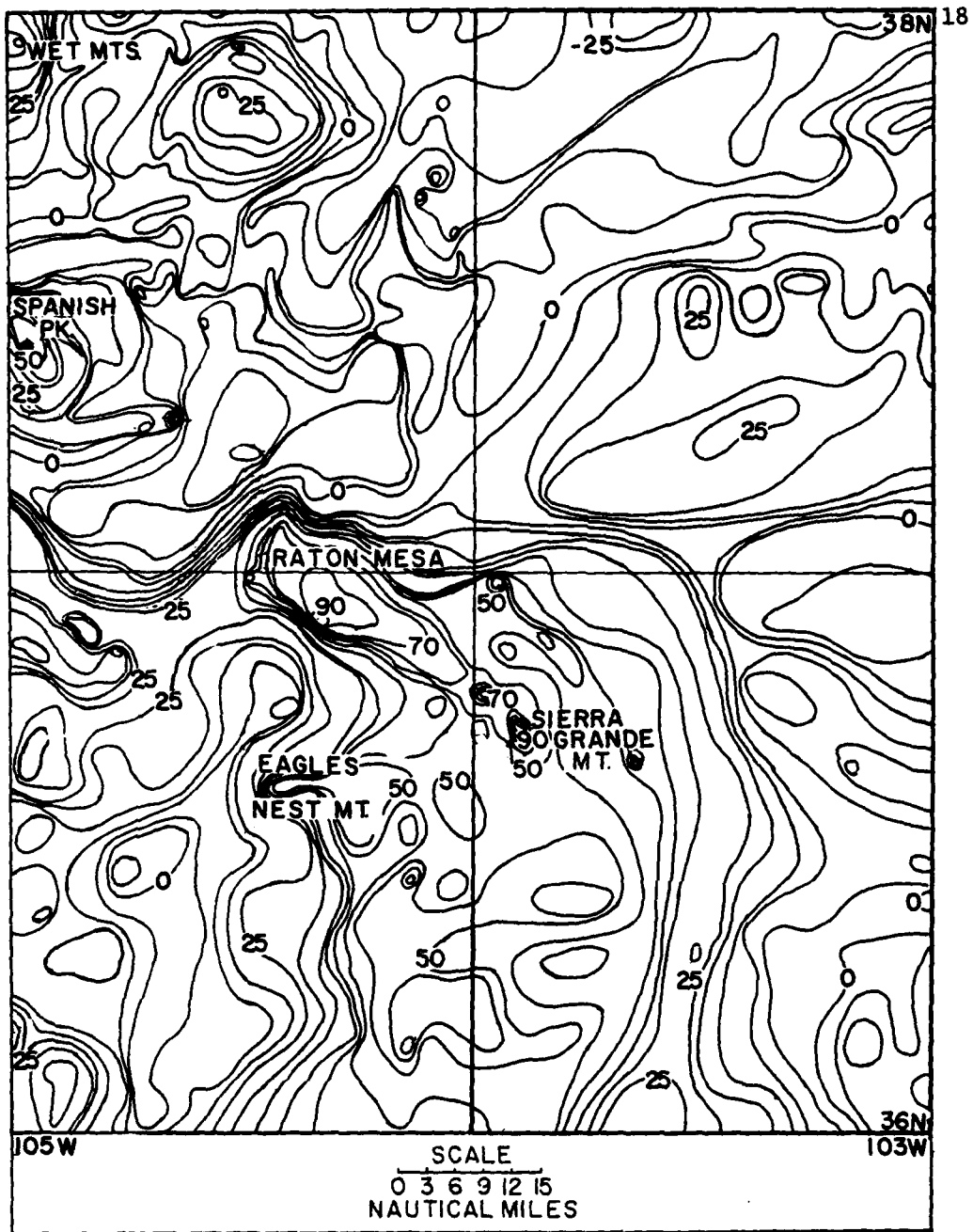


Figure 4. Regional free air gravity map using NOAA gravity data. Datum is sea level and gravity stations are shown in Figure 10. Contoured by hand.

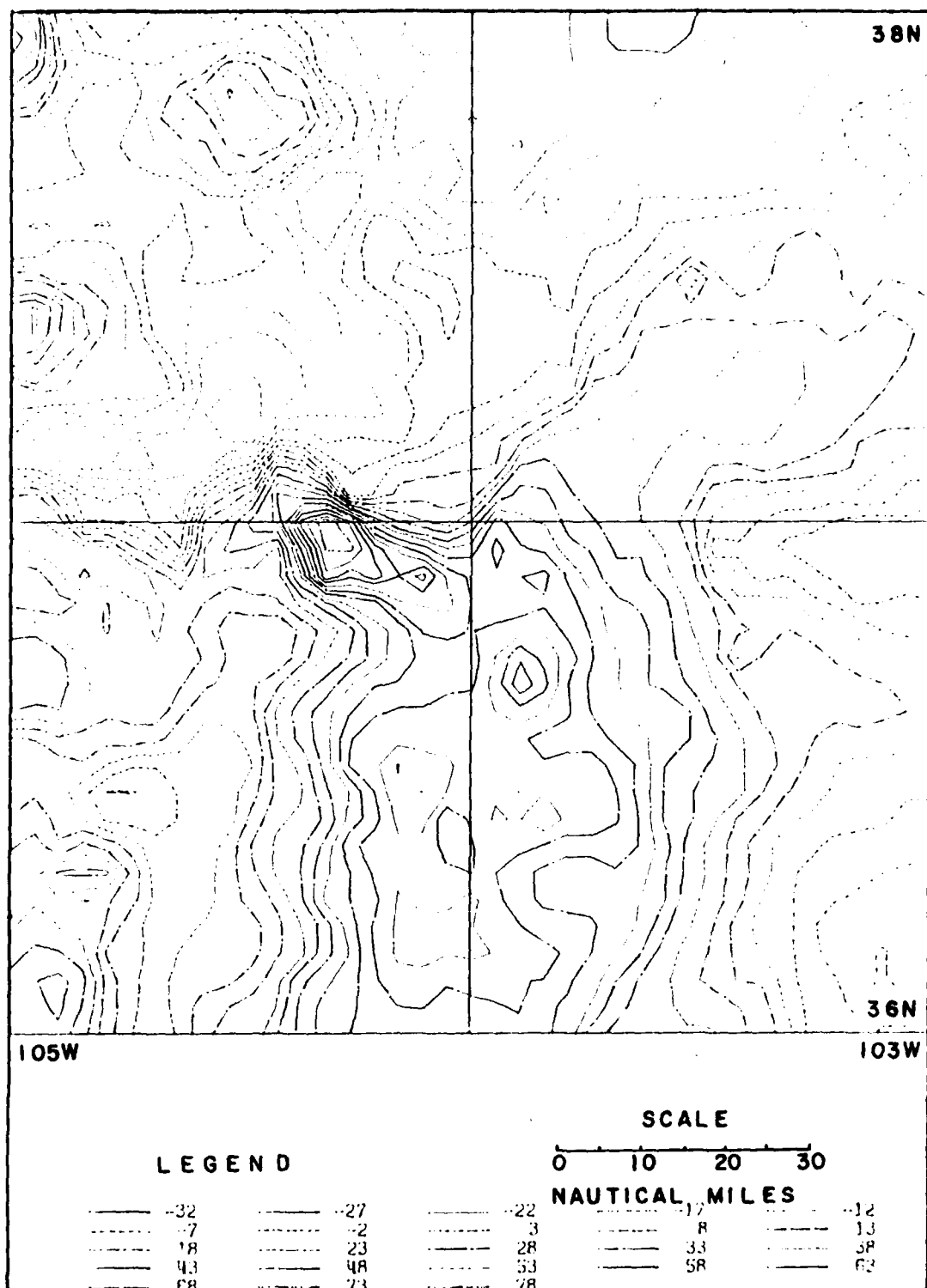


Figure 5. Regional Free Air anomaly map of the study area. Gravity stations are the same as in figure 10. Contour interval is 5 mgal, datum is sea level.

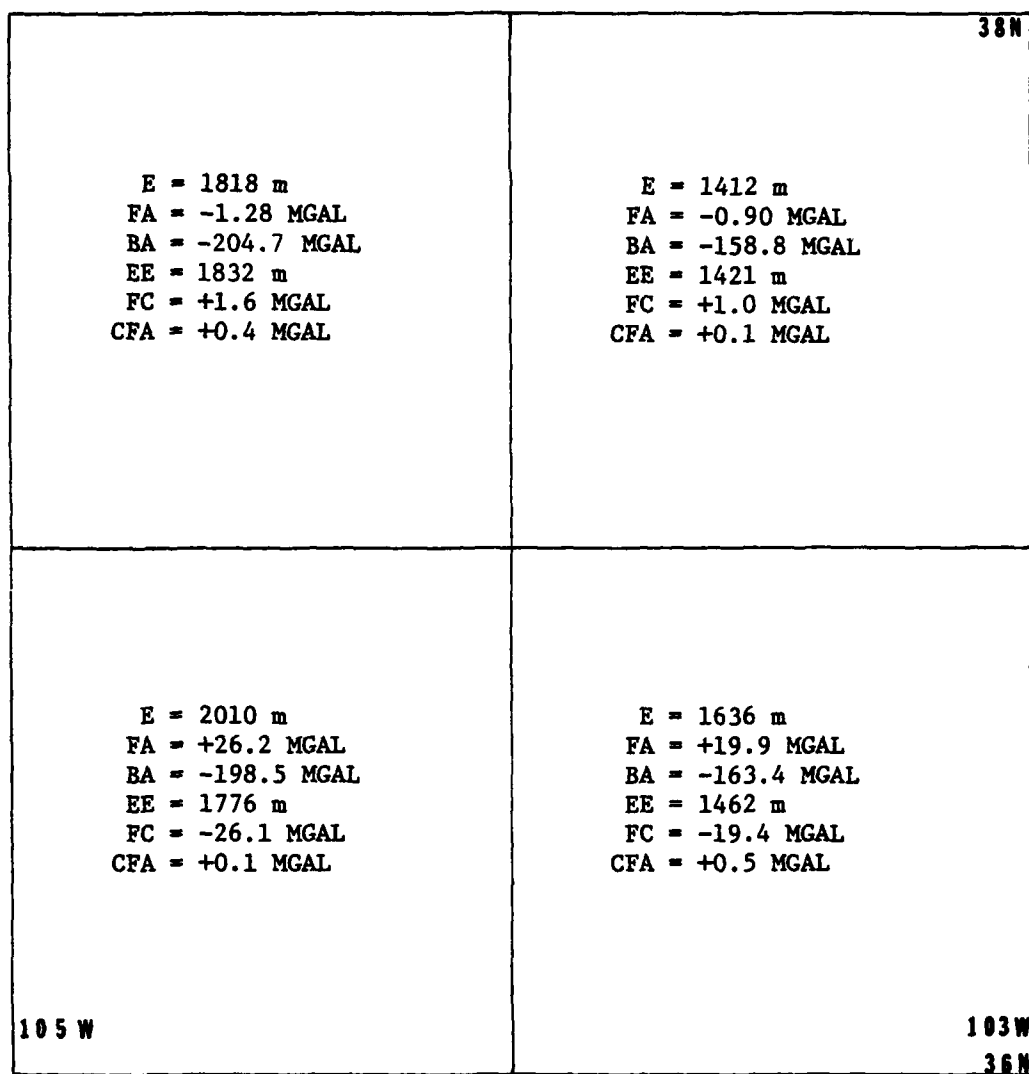


Figure 6. Graphic representation of the algebraic averages of the NOAA gravity and elevation data divided into one degree latitude and longitude blocks. E = elevation; FA = free air anomaly; BA = Bouguer anomaly; FC = Faye correction; EE = equivalent elevation; CFA = corrected free air anomaly (FA + FC).

measurement, of the near surface rock (the positive mass) is larger than the gravitational effect of the negative mass at the compensation level simply because the near surface rock is nearer the measured station. This means that a positive free air anomaly is in part caused by depth to compensation and does not necessarily indicate crustal loading. It is possible that the total observed free air anomaly can be explained in terms of the depth of isostatic compensation. Therefore, if the free air anomaly is to be used in an estimation of isostatic adjustment, a correction must be applied.

The correction applied to the observed free air anomaly for the effect of depth to compensation is generally called the Faye correction, after the man who first discussed the effect in the Nineteenth Century. One method of calculating the Faye correction uses the Bouguer anomaly to determine the elevation of the surface of a slab which is in isostatic balance (Woollard, 1962). This is done by assuming, if isostatic adjustment is complete, the Bouguer anomaly is related to the surface elevation of the crustal load causing the adjustment. The elevation of this surface slab is thought of as the equivalent elevation ( $h'$ ) derived from the Bouguer anomaly ( $h' = BA/2\pi\gamma\rho$ ; where  $\gamma$  is the gravitational constant and  $\rho$  is the assumed density). The equivalent elevation is subtracted from the station elevation ( $h$ ) and the difference ( $\Delta h$ ) defines the slab thickness used in the Faye correction (F.C.):  $F.C. = 2\pi\gamma\rho\Delta h$ . The Faye correction is subtracted from the free air anomaly to produce a corrected free air anomaly value, which is actually the isostatic anomaly since this computation has removed the effect of depth of compensation upon

the free air anomaly. As a result of applying the Faye correction to the free air anomalies in the study area (figure 6) the corrected free air anomalies clearly suggest regional isostatic equilibrium.

Although regional isostatic equilibrium is established, the locally positive average free air anomalies of the southern two blocks (figure 6) are indications of a lack of local compensation. The Quaternary volcanic rock covering most of the southern two blocks of the study area is missing in the northern portion of the study area and is assumed to be the cause of the large positive free air anomaly in the southern two blocks. If this is so, the free air anomaly can be used to estimate the rock thickness. If a density of 2.67 g/cc is assumed for the volcanic rock, and the formula for the gravitational effect of a slab is solved, a thickness of 180 m is indicated for the Quaternary volcanic rocks. As a confirmation of the rock thickness calculated from gravity data, a water well at Capulin National Monument penetrated 196 m of volcanic rock. The real thickness is probably somewhat irregular, and the value computed from the gravity data appears to be a good estimate.

Comparison of the free air map and topographic map (figure 7) shows that positive topographic features are also areas of positive free air gravity anomalies throughout the Basin and Great Plains. This relationship is to be expected (Woollard, 1959), and the larger topographic features are associated with larger local positive free air anomalies.

The area of the Capulin free air gravity map (figure 8) is covered by volcanic rocks of three sequences - Raton, Clayton, and Capulin. The average free air anomaly over the map is about +55 mgal, with a large

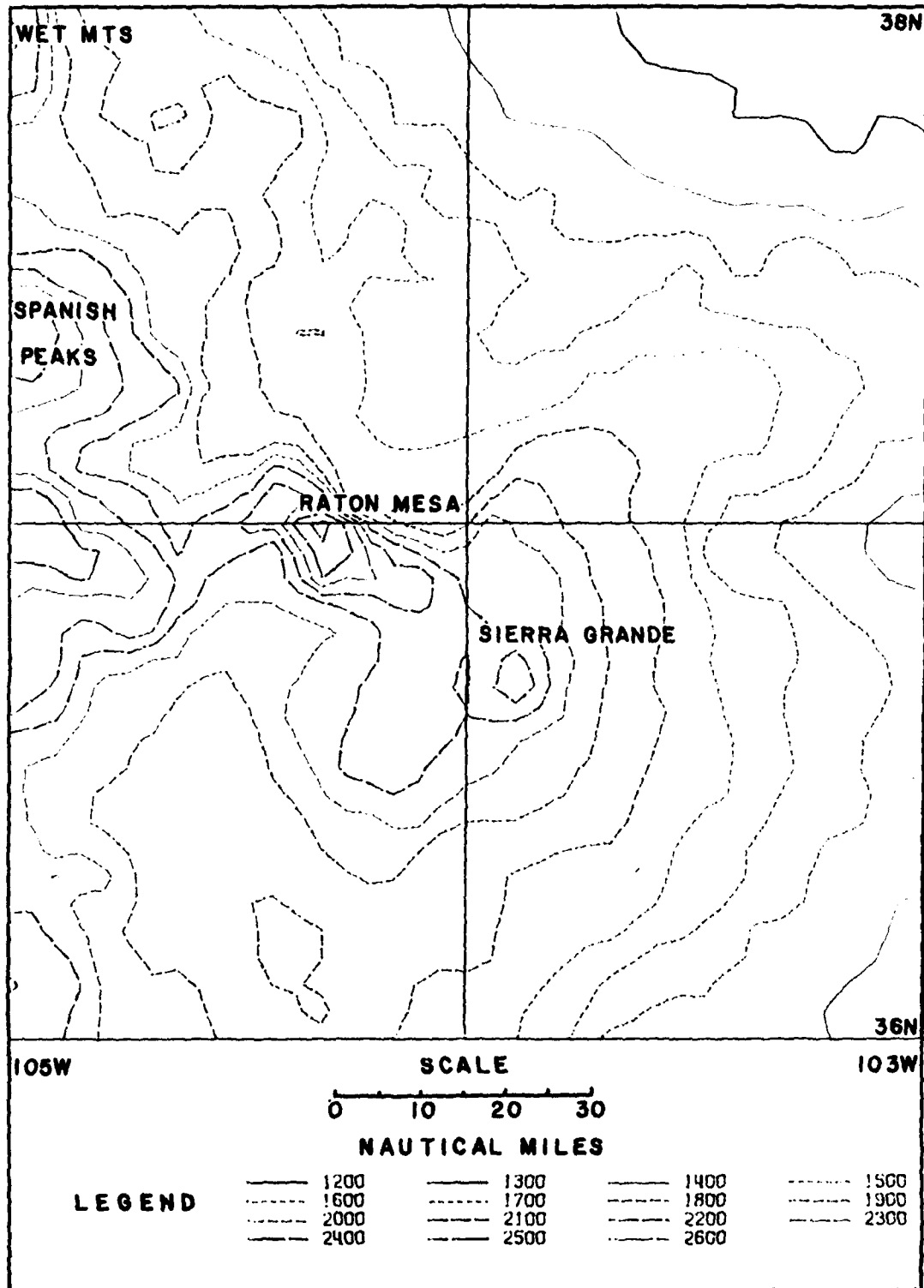


Figure 7. Regional topographic map of the study area. Contoured in meters, datum is sea level.

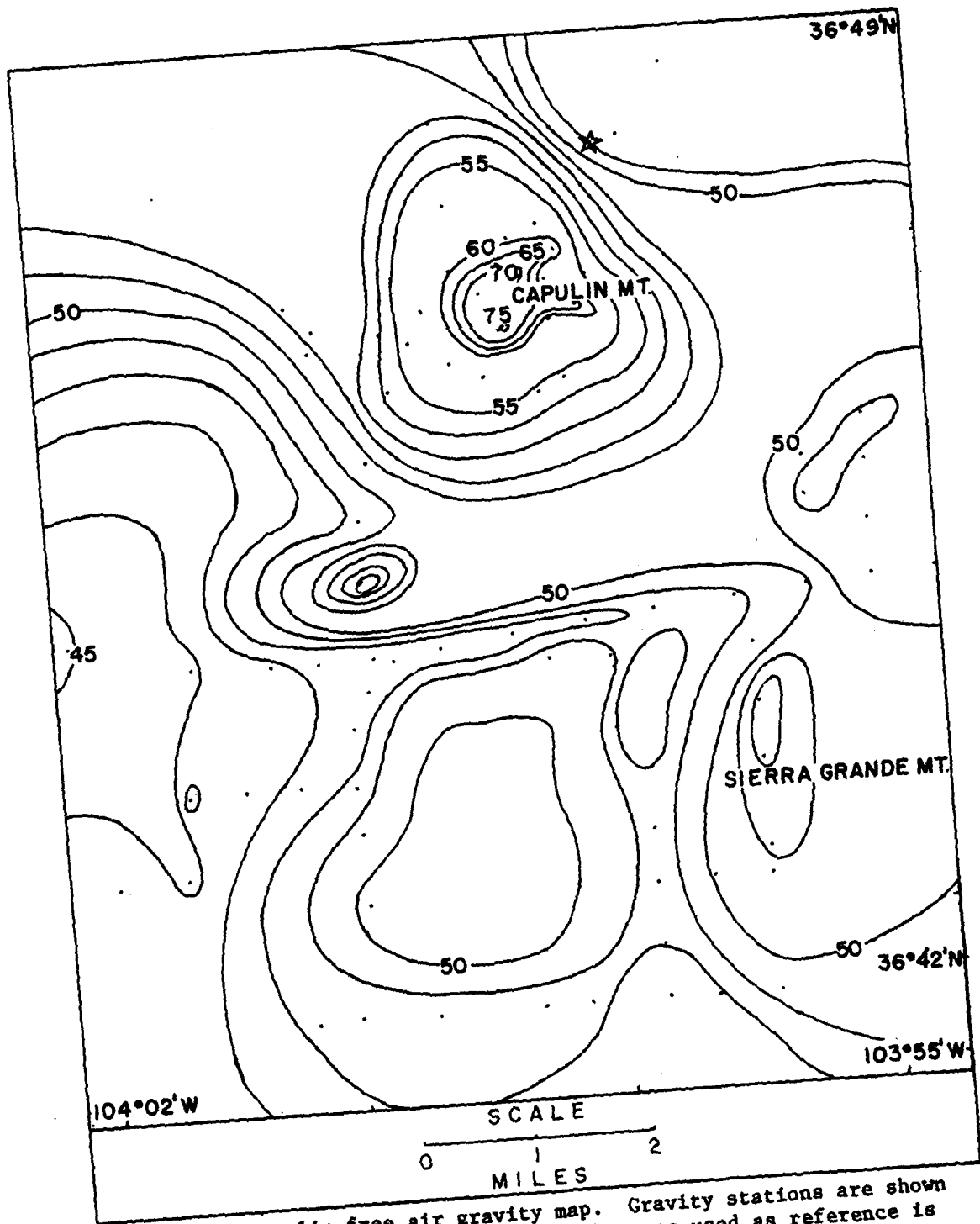


Figure 8. Capulin free air gravity map. Gravity stations are shown by dots (·), and station number one used as reference is designated by a star. Station number one is also a NOAA gravity station, therefore, correlating the Capulin gravity data to the NOAA gravity data.

free air anomaly of +70 mgal associated with Capulin Mountain. This large free air anomaly at the mountain station (+70 mgal) is +15 mgal different than the regional free air value immediately around the mountain (+55 mgal). The 335 m cone comprising the mountain has approximately the same volume as a right cylinder 112 m high with the same radius of 500 m. The gravitational effect of such a cylinder, assuming a density of 2.67 g/cc, would be 12.4 mgal if the top of the cylinder is located at mountain peak elevation. This calculated value is not precisely equal to the 15 mgal anomaly observed associated with Capulin Mountain, but the method of calculation is only approximate. Agreement is close enough to allow the assumption that the gravitational effect of Capulin Mountain itself is 15 mgal.

#### Bouguer Gravity Data

The plot of average elevation against average Bouguer anomalies (from figure 6) indicates an inverse relationship between elevation and the Bouguer data (figure 9). The Bouguer anomaly is actually the negative gravity effect of the root increment below the compensation level. As the terrain elevation increases, the root increment below the compensation level also increases in thickness to maintain isostatic equilibrium. An increase in the thickness of the root below compensation level results in a more negative Bouguer anomaly. The Bouguer gravity maps (in hand drawn form - figure 10, and computer plotted form - figure 11) indicate this relationship between rising topography (figure 7) and a decreasing Bouguer equipotential surface. The slab assumed in making the Bouguer correction results in the computation of a Bouguer anomaly that is excessively negative in areas which are distinguished

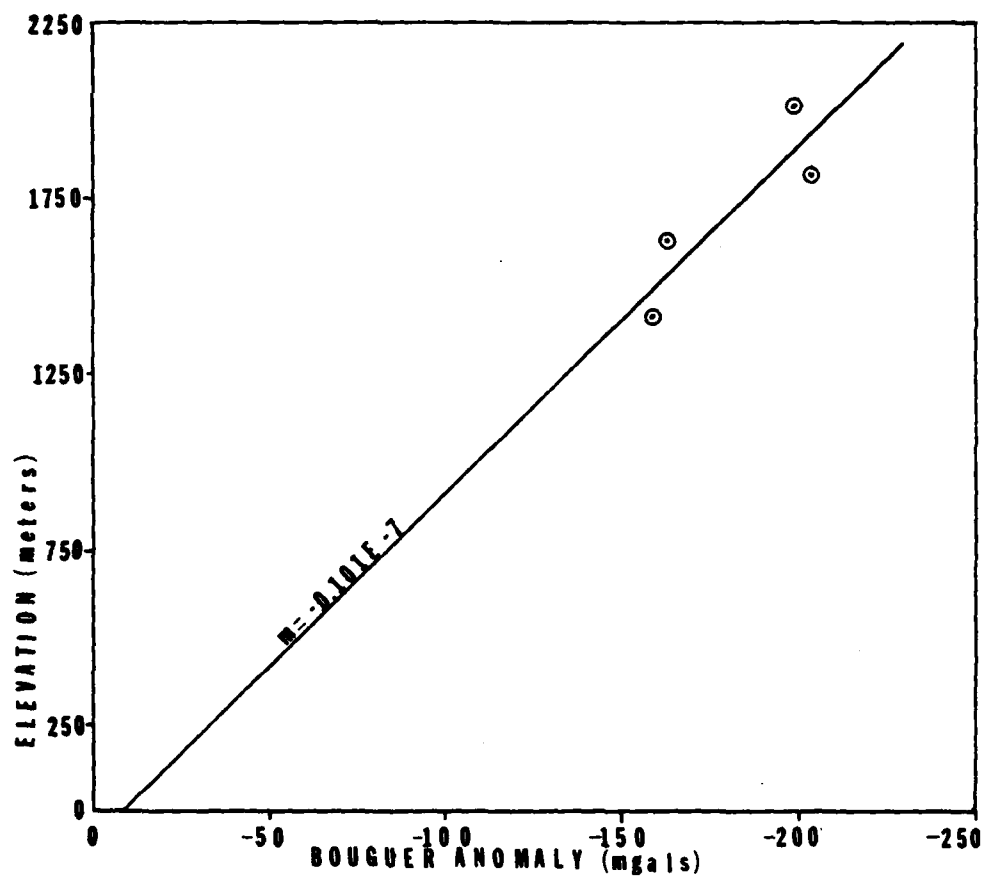


Figure 9. Plot of the averaged NOAA elevation data vs, the averaged NOAA Bouguer gravity data. The slope of the line,  $m$ , shows the inverse relationship of elevation and Bouguer gravity values.

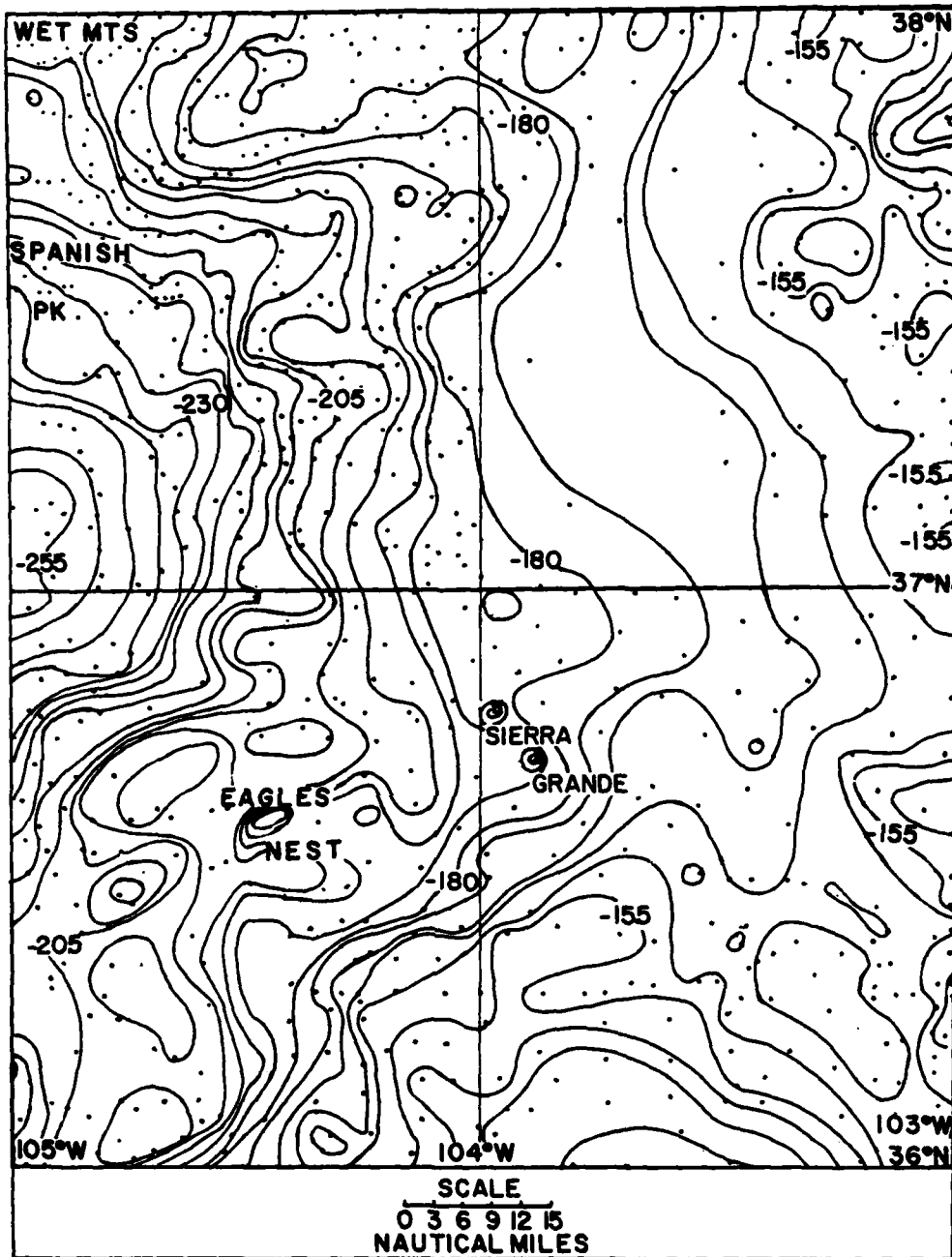


Figure 10. Regional Bouguer gravity map using NOAA gravity data. The dots represent the gravity stations. Datum is sea level, and a density of 2.67 g/cc was used in calculating the Bouguer correction.

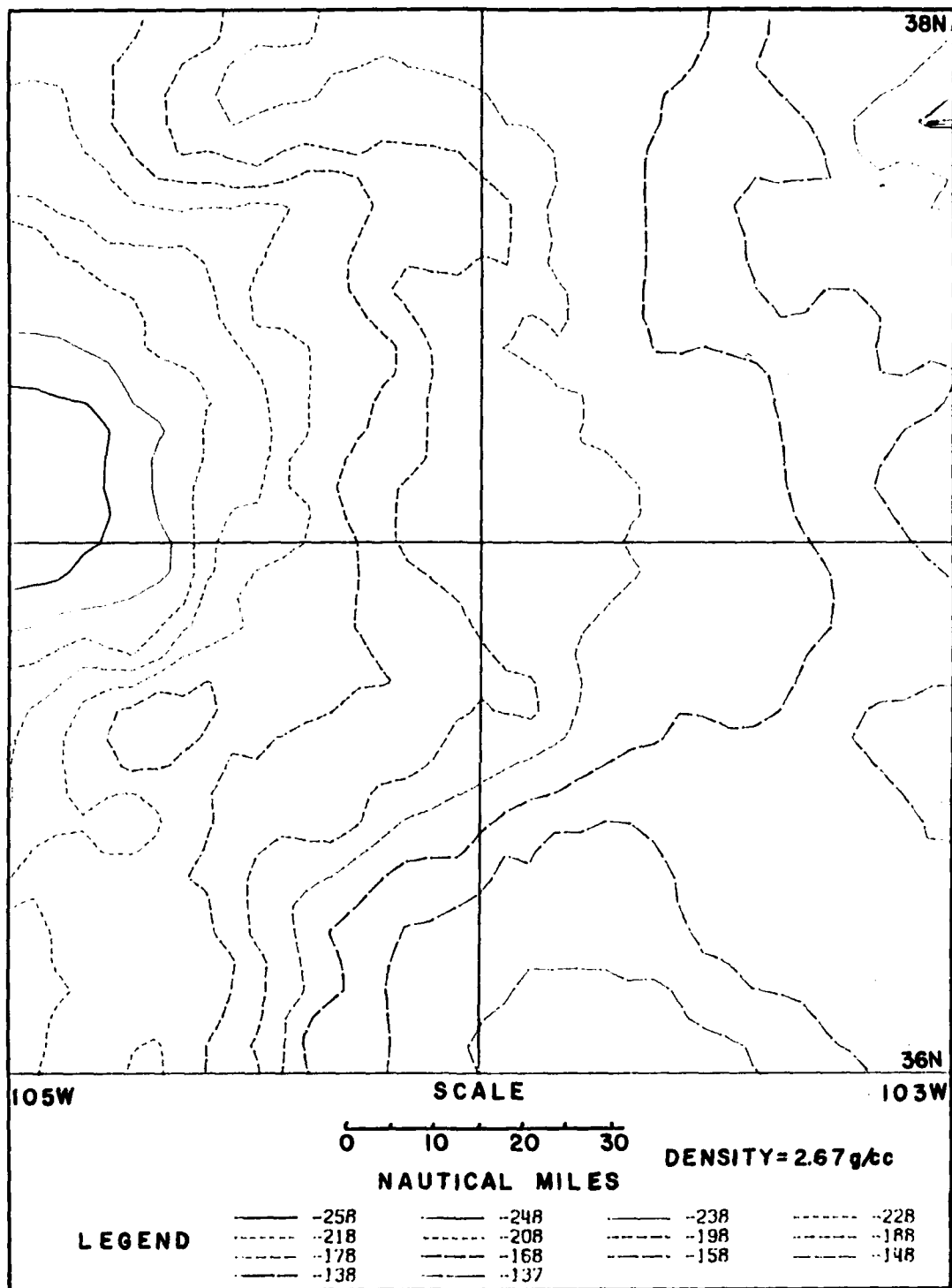


Figure 11. Regional Bouguer anomaly map of the study area. Gravity stations are the same as in figure 10. Contour interval is 10 mgal, datum is sea level.

by topographically isolated terrain, such as mountains. Sierra Grande Mountain is an example of this effect; however, Spanish Peaks and the Wet Mountains regions have sufficient areal extent to allow the slab assumption in the Bouguer calculation.

Eagles Nest Mountain has associated with it both a positive free air anomaly and positive relief with respect to the surrounding Bouguer surface on the Bouguer anomaly map. The positive free air anomaly is expected due to the near surface mass effect of the mountain. The presence of positive relief on the Bouguer equipotential gravity surface may indicate a near surface high density body, which would cause the Bouguer correction to be too small, or it may indicate the extension below datum of the igneous material forming the mountain. In either case, it appears that the density of the rocks forming Eagles Nest Mountain is greater than 2.67 g/cc.

The free air anomalies corrected for the Faye effect in the study area have already been shown to indicate isostatic adjustment, and the computation of isostatic anomalies directly from Bouguer anomalies can be used to add validity to this conclusion. The computation of the isostatic anomalies done here is based upon the Airy isostatic model with the density contrasts and formulas suggested by Woollard (1969). The slab thickness of the mass below the compensation level is determined by assuming that part of the negative Bouguer anomaly is caused by the presence of a slab of crustal material displacing heavier mantle material. Woollard (1969) determined that a crustal density of 2.92 g/cc is representative of the crustal rock at the compensation level (M-discontinuity)

and a density of 2.67 g/cc is representative of the upper crustal rock. The gravitational effect of the elevated surface is equal to the simple Bouguer correction computed using a density of 2.67. However, the effect of the surface slab upon a measured value on the surface is exaggerated as compared to the effect of the compensating root slab upon the same measurement as previously discussed. Therefore, if the region is in isostatic balance, the observed simple Bouguer anomaly is equal to the Bouguer gravity effect computed for the surface slab with average elevation in the area, minus the exaggeration effect of slab position. Previously, it was shown that this exaggeration effect is approximately equal to the observed free air anomaly. The isostatic anomalies for each one degree block in the study area have been calculated in this manner, and the values are shown in table 1.

These isostatic anomalies show the study area to be in near isostatic equilibrium, as was suggested in the free air anomaly discussion. Qureshy (1962) studied the Bouguer data for all of Colorado and concluded that the eastern portion of the state, including the northern part of this report's study area, is in isostatic equilibrium. The slight positive bias in the results may be explained by either crustal thickening or increased crustal density (Woollard, 1969).

Table 1 includes calculations of crustal thickness using Shurbet's (1966) density model and formulas. The crust thins from west to east, and continues to thin east of the study area. Stewart and Pakiser (1962) calculated a seismic refraction profile using the Gnome explosion. Their computed thickness is very close to the crustal thicknesses

Table 1. Theoretical and actual gravity anomalies in the study area. All values averaged over one degree block.

Area $10^{\circ}10'$ N-W	Elevation h (meters)	Theoretical gravity due to the posi- tive mass $g_p$ mgal (2)	Obs. BA $p=2.67$ g/cc mgal (1)	Obs. FAA mgal	Isostatic anomaly FA-BA-gp	Compensation "root" H km (3)	Crustal thickness T km (4)
36-103	1636	182.8	-163.4	+19.9	+0.5	9.07	43.71
36-104	2010	224.6	-198.5	+26.2	+0.1	11.02	46.03
37-103	1412	157.8	-158.8	-0.9	+0.1	8.82	43.23
37-104	1818	203.1	-204.7	-1.2	+0.4	11.37	46.19

(1) from figure 6

(2)  $g_p = 2\pi\rho h$ , where  $\rho = 2.67\text{g/cc}$ , and  $h =$  average terrain elevation

(3) from Shurbet (1966)  $H = BA/2\pi\rho p = BA/18.01$ , where H is the thickness of the compensation root;  $\rho = 2.67\text{g/cc}$

(4) from Shurbet (1966)  $T = 33 + H + h$ , where T is crustal thickness, H is root thickness, and h is terrain elevation

calculated using gravity data in this report.

In addition to the NOAA Bouguer gravity data, a separate Capulin Bouguer gravity map (figure 12) was prepared from data collected by the author. The Bouguer anomaly associated with Capulin Mountain is about -200 mgal, which is approximately 20 mgal more negative than the adjacent area. Since the mountain is a feature with little area, the slab assumed in the Bouguer correction has exaggerated the Bouguer anomaly. Because the mountain itself is 335 m high, a total of 37.4 mgal was subtracted from the measured value as a part of the total Bouguer correction for the height of the mountain. The actual gravitational effect of the mountain has previously been shown to be about 15 mgal. Therefore, the Bouguer correction applied to the mountain station was exaggerated by 22.4 mgal. Correction for this exaggeration shows the area beneath the mountain to be only slightly more negative than the surrounding area, and no additional mass deficiency exists beneath the mountain as compared to the surrounding area.

Since the study area, including the Capulin area, has been shown to be in isostatic balance, the Bouguer equipotential surface is expected to reflect variations in crustal thickness as well as local changes in crustal density. Therefore, the Bouguer anomalies can be used to calculate sedimentary thickness in the Basin. Calculations of this kind were carried out to produce a basement relief or structure map.

#### Raton Basin Basement Structure Map

In previous studies (Griggs, 1948; Baltz, 1965), subsurface structure in the Basin has been deduced from surface rocks and well log

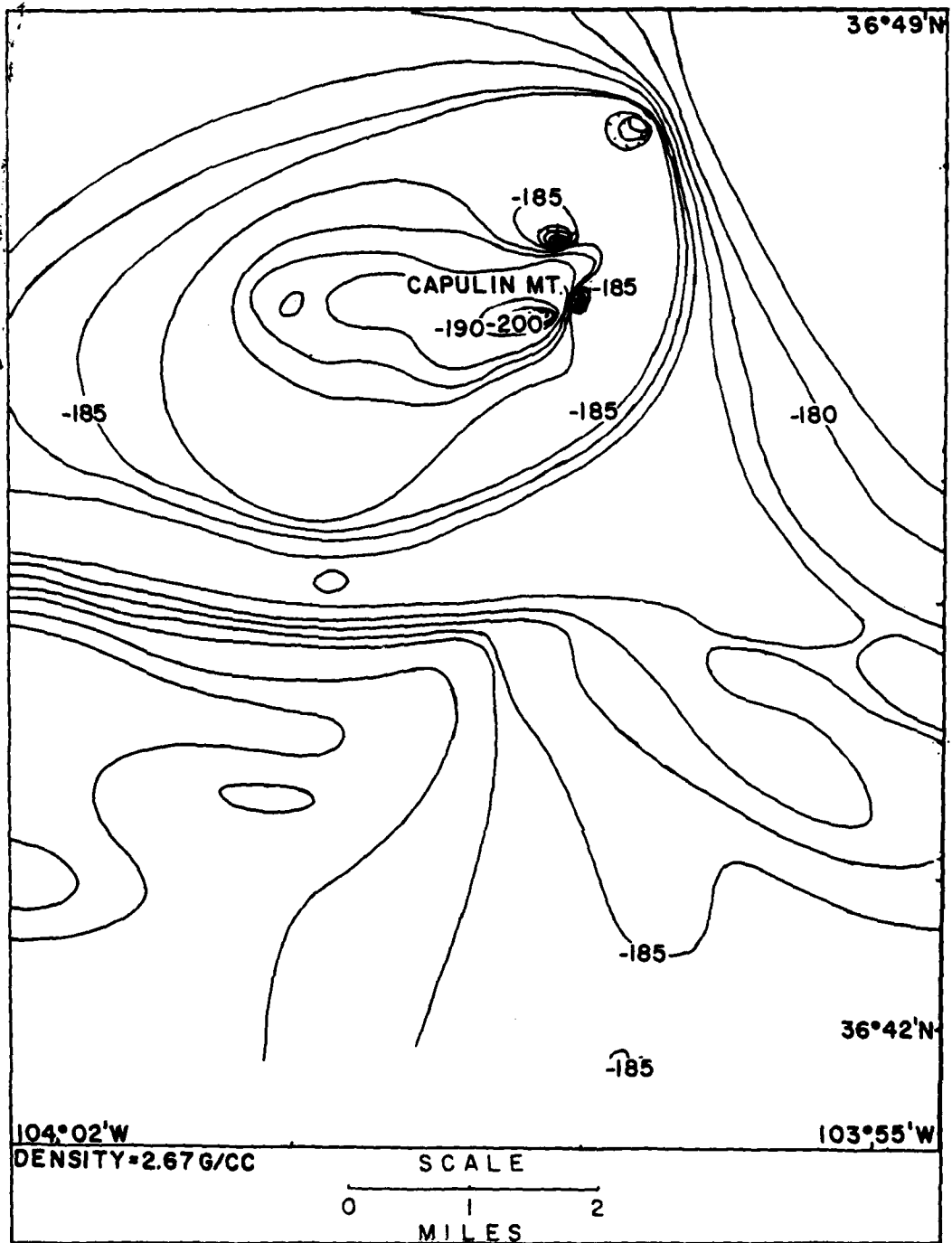


Figure 12. Capulin Bouguer gravity map. Data stations are the same as shown in Figure 8. Density used for the Bouguer corrections is 2.67 g/cc.

data. A basement relief map based on structural data cannot be drawn because geologic mapping in the Basin is incomplete. However, Bouguer gravity data were used in this study to deduce crustal thicknesses and to determine basement structure (or relief). The basement surface computed is defined as the boundary between the less dense sedimentary rocks above and denser crystalline rocks below. Intrusive rocks that penetrate the strata are also classified as basement rocks because their presence causes effective thinning of the sedimentary column in the computation.

The best method for determining basement relief is based upon the realization that the Bouguer anomaly is actually the negative gravity effect of the slab or root which has displaced the heavier material of the sub-compensation level. In this study, it is assumed that the negative effect is locally affected by less dense sedimentary rocks displacing heavier basement rocks; therefore, the variation in the Bouguer gravity values can be interpreted in terms of variation in the thickness of the sedimentary rocks.

As a first step in constructing a basement relief map for the Basin it was necessary to ascertain the regional trend of the Bouguer gravity map. A second order polynomial surface was empirically determined to best represent the Bouguer gravity surface as discussed in Chapter II. Variation between this regional trend and the observed local Bouguer gravity values is assumed to be caused by differences in thickness and density of the sedimentary rocks.

The areal extent of the various lithologic units is shown in plate

1; Clark (1966) gives representative densities for the rock types present. Representative densities for the columnar sections (figure 3) for the Las Vegas and Raton Basins, respectively, were found to be 2.27 g/cc based on the densities reported by Clark (1966). The density contrast between the representative density for the Basin and the density used in the Bouguer correction (2.67 g/cc) is -0.4 g/cc. Estimations of lateral variations in the density contrast throughout the Basin were based on the following criteria: 1) sedimentary rock thinning near the Apishipa, Cimarron, and Sierra Grande Arches; 2) presence of volcanic rock in the southern portion of the Basin; 3) higher density intrusive rocks near Spanish Peaks and Wet Mountains regions; and 4) an average sedimentary rock density of 1.8 g/cc (producing a -0.87 g/cc density contrast) for the Great Plains (east of the Apishipa Arch - Sierra Grande Arch axes) as determined by Shurbet (1966). A representative calculation from the Bouguer gravity map (figure 10) along  $37^{\circ}\text{N}$ ,  $104^{\circ}$ - $105^{\circ}\text{W}$  is included (figure 13).

At  $37^{\circ}\text{N}$ ,  $104.5^{\circ}\text{W}$  (figure 13), the Bouguer anomaly value, determined from the Bouguer gravity map, is -216 mgal. The regional Bouguer trend value (-210 mgal) was computed from a second order polynomial surface described in Chapter II. The residual gravity value ( $\Delta g$ ) at  $37^{\circ}\text{N}$ ,  $104.5^{\circ}\text{W}$  is the difference between the Bouguer gravity value and regional trend value at that point (-210 + 216 mgal = +6 mgal). The density contrast value ( $\Delta \rho$ ) at  $37^{\circ}\text{N}$ ,  $104.5^{\circ}\text{W}$ , determined from the density contrast model, is -0.58 g/cc. The depth to the basement relief surface is found

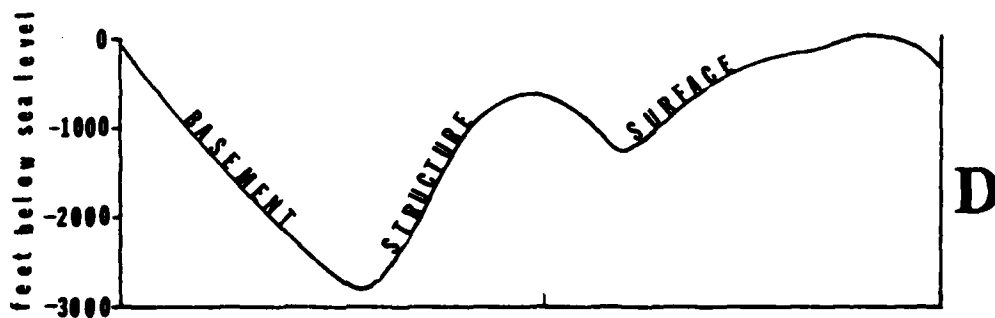
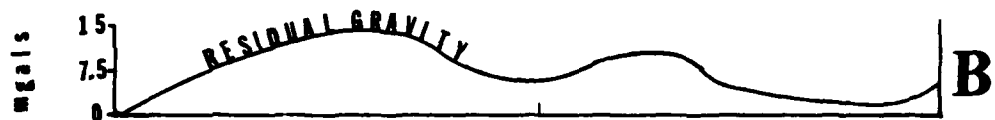
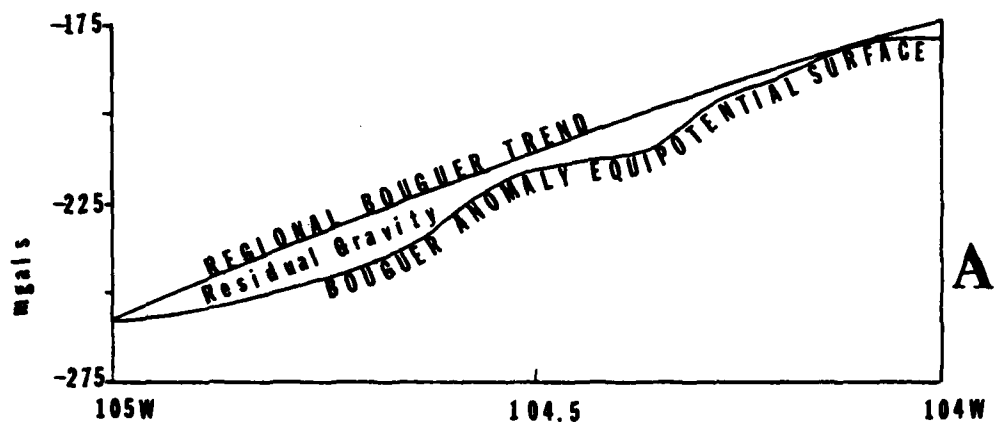
Figure 13. Basement structure profile derived from NOAA Bouguer gravity data along 37°N, 104°-105°W.

A. The regional Bouguer dip is determined by a smooth curve through the Bouguer anomaly equipotential surface.

B. The difference of the regional Bouguer dip from the Bouguer anomaly equipotential surface in A is known as the residual gravity ( $\Delta g$ ).

C. The density contrast model ( $\Delta \rho$ ) is constructed from the known densities of the stratigraphic units in the Basin and subtracting those densities from the 2.67 g/cc density used in the Bouguer correction. Since the sediment density is 1.8 g/cc and it is assumed that the sediments are displaced crustal rock ( $\rho = 2.67$  g/cc), the gravity effect of this displacement is negative.

D. The depth to the basement structure surface ( $h$ ) is calculated by using  $\Delta g$  from B and  $\Delta \rho$  from C above in the gravity mass effect formula:  $h = \Delta g / 2\pi\Delta\rho\gamma$ .



by solving the gravitational effect formula for depth (h), using the  $\Delta g$  and  $\Delta \rho$  values above:  $h = \Delta g / 2\pi\gamma\Delta\rho = -810$  feet (below sea level). This type of calculation was repeated for each of the 2,400 density contrasts in the Basin, and the resulting depths to basement structure were then contoured by the computer techniques described in Chapter II. The accuracy of the depths to the basement structure surface was independently verified using well log data (Baltz, 1965) and a measured section from the Raton Basin (McGehee, 1955).

In order to describe the correlation between the geology on plate 1 and the basement structure on plate 2, the same topographic names are used to refer to features on both maps. This practice is justified because the features named on the basement structure map all have associated topographic features. In the area of the Wet Mountains and Spanish Peaks, the basement structure map shows that basement rock is exposed; that is, there are no sedimentary rocks present. The structurally high Apishipa Arch area on the basement relief map extends southeast of the Wet Mountains. The basement rises at about  $1.5^\circ$  to approximately 1,500 feet of vertical relief over a ten mile distance. The Apishipa Arch area is outlined by positive relief for approximately 50 miles on the basement structure map. The basement structure map shows the Apishipa Arch as the eastern boundary to the Basin.

The Delcarbon and La Veta syncline areas are shown on the basement structure map as depressions. The Delcarbon depression is above sea level and the La Veta depression is below sea level; both depressions

deepen to the south. The axis of the La Veta depression is the deepest depression on the basement structure map and defines the Raton Basin axis.

A positive relief feature on the basement relief map between the La Veta and Delcarbon depressions is also associated with intrusive rocks on the geologic structure map (plate 1). The shallow depth to known oil bearing formations of Cretaceous age (Baltz, 1965) make this anticline a favorable site for petroleum exploration. However, the heat from the intrusive activity may have destroyed any oil present, in a manner similar to the destruction of coal beds found elsewhere in the Basin and described in Chapter I.

The Cimarron Arch is an area of positive basement relief and clearly separates the Raton and Las Vegas Basins. It is asymmetric in shape, steeper on the north slope ( $4.5^{\circ}$ ) than the south slope ( $2.9^{\circ}$ ), and has approximately 3,500 feet of vertical relief. The Cimarron Arch area extends about fifty miles, from the west edge of the basement structure map to the Sierra Grande Arch area. The marked relief of this basement feature suggests the Arch has effectively prevented intertonguing of Las Vegas and Raton Basin's sedimentary rocks. As the Basins were downwarped and isostatic adjustment occurred to compensate for the accumulating sediments, the Cimarron Arch remained a positive structural feature. Although not a significant topographic or gravity feature today, the Arch was important in the development of the Basin.

The Sierra Grande Arch area is roughly defined by moderate relief on the basement structure map for approximately twenty miles east of

the Las Vegas Basin. Total positive relief increases about 1,000 feet over a twelve mile distance, producing a gentle  $0.8^{\circ}$  slope. The whole eastern sector of the basement structure map is a low relief positive area, rising slowly to the Apishipa and Sierra Grande Arch areas.

A previously unmapped and unnamed basement trough, which is in near alignment with a left lateral fault south of Spanish Peaks (plate 1), trends northeast from Raton Basin toward Apishipa Arch. The trough deepens southeast, towards the Raton Basin, and may be fault controlled. As a structurally low feature, the unnamed trough may contain significantly more sediments than areas surrounding it. The margins of the unnamed trough may prove favorable for future petroleum exploration. Presence of this trough is confirmed on the Raton Basin magnetic map.

#### Raton Basin Magnetic Map

The Raton Basin vertical magnetic data is tabulated and included in Appendix C. The magnetic data is shown in both hand drawn (figure 14) and computer plotted formats (plate 3). The computer plotted magnetic map is drawn at the same scale as the basement structure map for comparison. Zeitz et al., (1969) showed that the Colorado sedimentary rocks in the Basin are essentially nonmagnetic, the metamorphic and volcanic rocks are weakly to moderately magnetic, and the Precambrian quartz monzonite rocks are moderately to strongly magnetic. The Raton Basin magnetic maps actually represent the surface of the basement rocks in the Basin. Magnetic anomalies may also be associated with lateral changes in rock types, but there is no geologic evidence for basement

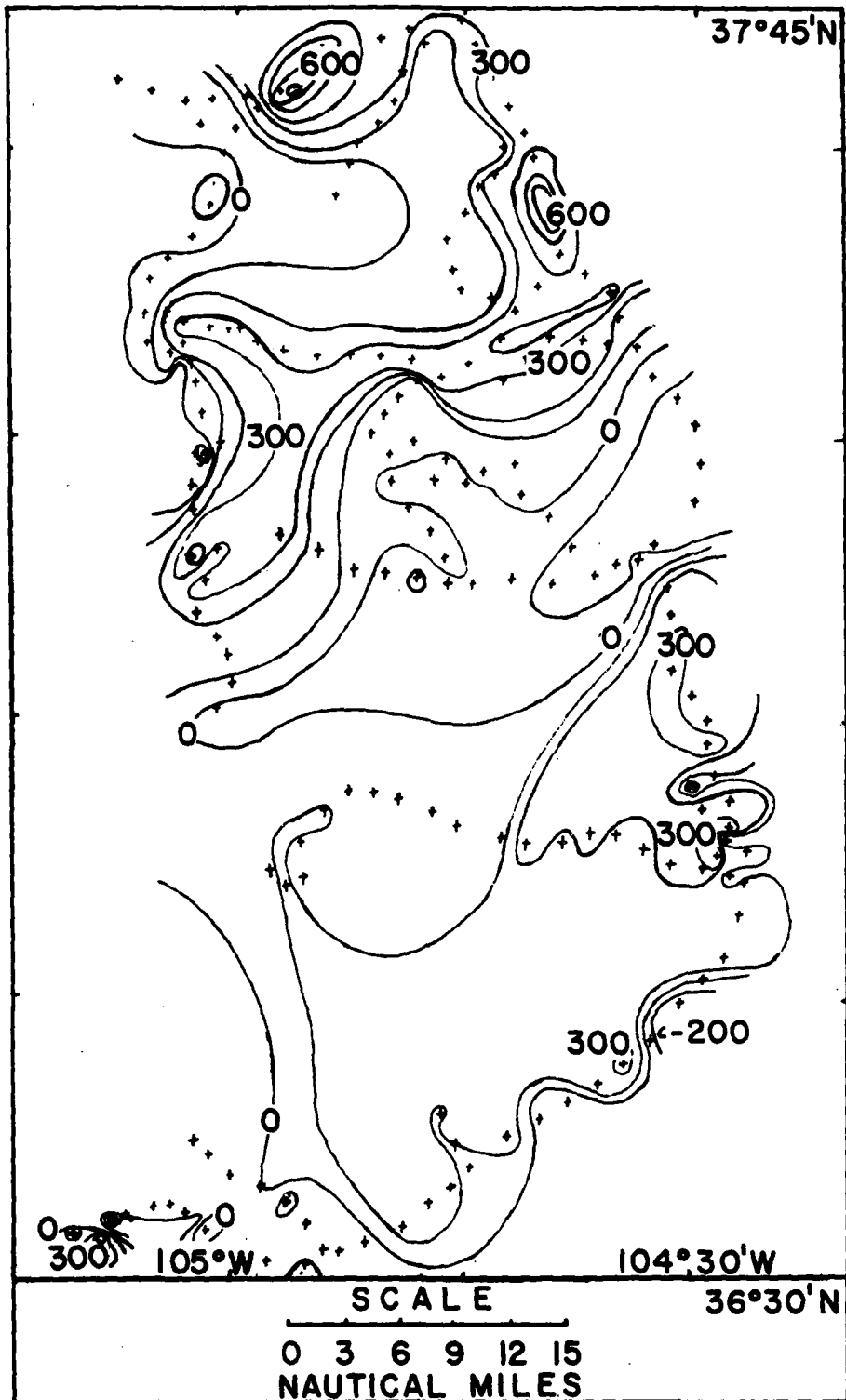


Figure 14. Raton Basin magnetic map. The crosses represent magnetic stations. Station number one is used as reference and is shown circled in the lower left corner of the map.

rock type changes in the Basin with the exception of those areas of known intrusive rocks.

Metasedimentary rocks are exposed near the Cimarron Arch and these rocks are near station number one, which was the magnetic survey datum. Magnetic measurements in the area of the metasedimentary rocks gave no indication that these rocks have higher magnetic susceptibilities than the sedimentary rocks in the Basin. Therefore, it is reasonable to assume that the rocks in New Mexico have the same magnetic susceptibilities that Zeitz et al., (1969) reported for Colorado rock types. Some lack of detail in the magnetic map in the southern portion of Raton Basin is the result of poor road access. All magnetic measurements were made along roads.

Structural depressions (plate 1) are associated with negative magnetic anomalies (plate 3) in the Basin. The La Veta and Delcarbon synclines both have distinct low magnetic anomalies associated with them; the unnamed trough detected on the basement structure map also has a distinct low magnetic anomaly associated with it. The magnetic anomaly associated with the unnamed trough makes it appear to deepen to the northeast, opposite the direction determined on the basement structure map. However, this apparent deepening probably reflects only the computer response to the lack of magnetic stations in the eastern part of the survey area.

Positive magnetic anomalies are associated with positive structural features. For example, the unnamed anticline between the La Veta and Delcarbon synclines has a significant positive magnetic anomaly

associated with it. The Cretaceous age sediments with known oil shows are only thinly buried near this anticline.

Capulin vertical magnetic data were also studied as an addition to the Raton Basin magnetic data. The Capulin data are tabulated and included in Appendix B with the Capulin gravity data. Unlike the sediment filled Raton Basin, the Capulin area is covered by volcanic rocks, which have significantly higher magnetic susceptibilities than the sedimentary rocks beneath. Some of the magnetic anomalies in the Capulin area (figure 15) are associated with topographic features. For example, there is a magnetic anomaly associated with Capulin Mountain. However, a positive magnetic anomaly on the east slope of the mountain is not associated with a topographic feature. Free air gravity anomalies also mark this area, and this anomaly relationship may be an indication of lateral vents or dikes.

Variation in the magnetic properties of different volcanic rock types (Dobrin, 1976) would be helpful in identifying magnetic anomaly patterns in volcanic regions. Indeed, the largest positive magnetic anomaly is near Sierra Grande Mountain; smaller but equally distinctive positive magnetic anomalies are near Capulin Mountain. The unusually high magnetic susceptibility of the Sierra Grande sequence (indicated by its magnetic anomaly) may be diagnostic of these volcanic rocks and aid in determining their areal extent.

#### Capulin Local Seismic Study

In addition to gravity and magnetic measurements, an effort was made to determine natural seismicity in the Capulin area. It was

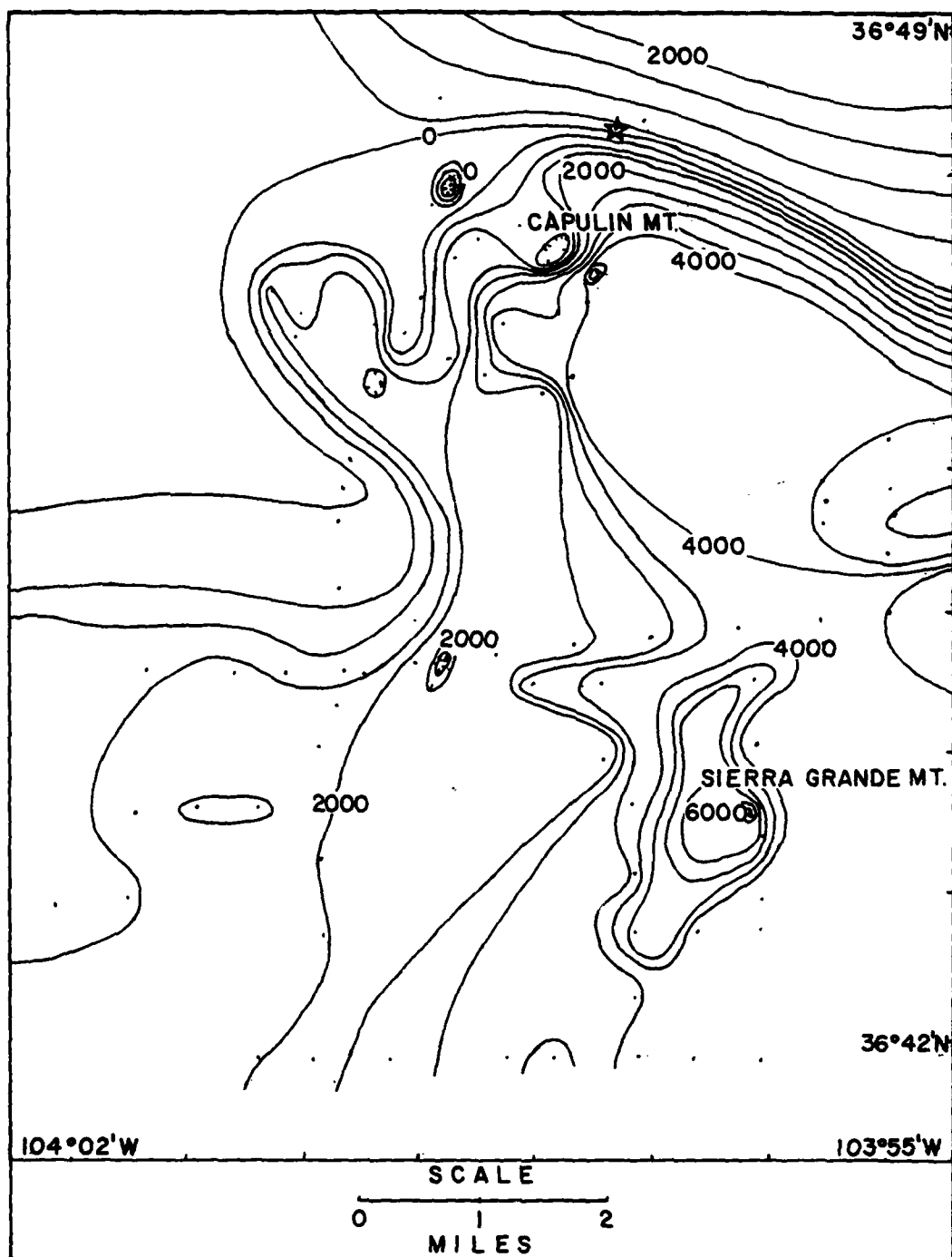


Figure 15. Capulin magnetic map. The dots represent magnetic stations. Station number one is used as reference and is represented by a star.

thought that some tectonic activity may be in progress. The results of the seismic survey in the Capulin area and all known seismic activity during the Twentieth Century are included in table 2. The epicenters of the earthquakes in table 2 are also shown on a map of northeastern New Mexico (figure 16).

A bar graph (figure 17) indicates the distribution of seismic activity in northeast New Mexico from 1900 to 1980. The lack of any significant recorded seismic activity during the first half of this century is due largely to the lack of recording equipment or populace to observe any shocks. Since 1962 the number of recorded events have increased due to the installation of permanent seismograph networks.

In the last five years seismic activity in New Mexico has declined (Sanford, 1981), yet this study suggests that the Capulin area has rather high seismic activity. The events recorded during this study were local in origin and small in magnitude, and were not recorded elsewhere

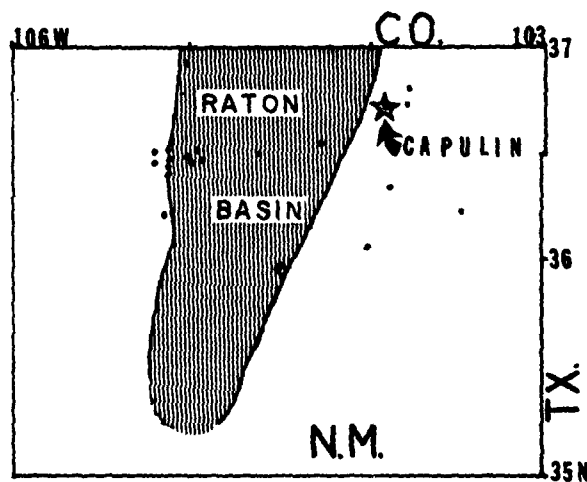


Figure 16. Geographic location of seismic events strong enough to be felt by local population in northeast New Mexico from 1900 to 1980.

Table 2. Recorded Earthquake Activity in the Study area of New Mexico 1900-1981.

SOURCE	DATE YR-MO-DAY	TIME GMT	LAT °N	LONG °W	INTENSITY modified Mercalli or local magnitude
1	06-04-19	2100	-	-	V
1	06-04-20	1300	-	-	VI
2	24-08-13	0423	36.0	104.5	V
2	52-08-13	2042	36.5	105.0	V
2	63-06-06	0806	36.6	104.4	2.7
2	66-09-24	0734	36.4	105.1	2.7
2	66-09-24	0827	36.4	105.1	2.4
2	66-09-25	1011	36.3	105.1	2.8
2	66-09-25	1223	36.5	105.1	2.8
2	72-02-20	2310	36.4	104.9	1.5
2	72-02-20	2323	36.4	104.9	2.2
2	75-05-16	0138	36.9	105.0	1.5
2	75-05-16	0726	36.5	104.7	1.9
2	75-06-21	0542	36.1	104.0	2.0
3	79-09-19	0539	36.4	103.7	1.8
3	80-09-12	2138	36.5	105.1	2.3
4	81-07-24	1613			
4	81-07-24	1815			
4	81-08-27	0220			
4	81-08-27	0238			
4	81-07-27	1554			
4	81-07-27	1738			
4	81-07-30	1824			
4	81-08-25	2034			
4	81-08-27	2041			
4	81-09-01	2124			
4	81-09-01	2254			
4	81-09-09	1724			
4	81-09-16	0336			

Source Data:

1. Anonymous, The Raton Range (April 21, 1906) shock felt at Folsom, NM
2. Sanford et al., (1981)
3. Sanford (1981)
4. Capulin data (this report) epicenters assumed at or near Capulin, NM. No intensities were calculated, but the sensitivity of the equipment would indicate the relative intensities to be much smaller than previously recorded in the area.

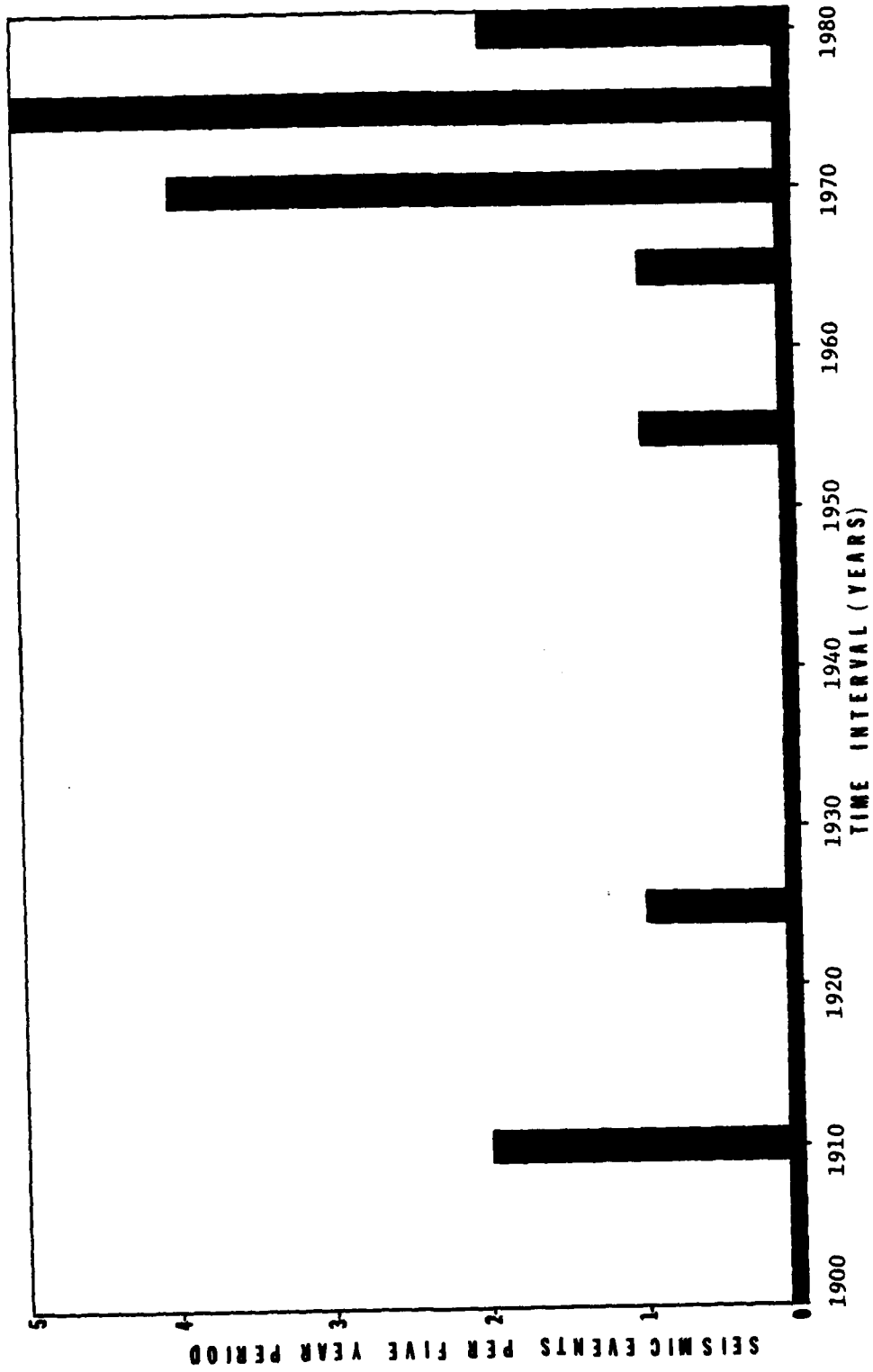


Figure 17. Bar graph representation of the frequency of seismic events in Table 2 in five year increments. Time interval is 1900 to 1980.

in the state (J.J. Wolff, personal communication, 1981). Some of the events recorded may have been local mining blasts or sonic booms, although sonic booms are usually easily distinguished (figure 18).

The presence of seismicity near Capulín suggests this area to be either affected by dormant vulcanism, or by tectonic adjustment along faults in the area. Sanford et al., (1981) suggest that seismic activity in northeast New Mexico may be due to an eastern extension of the Jemez Lineament in western New Mexico. Continued monitoring of the Capulín seismicity would be necessary to determine the source and extent of the local seismic activity.

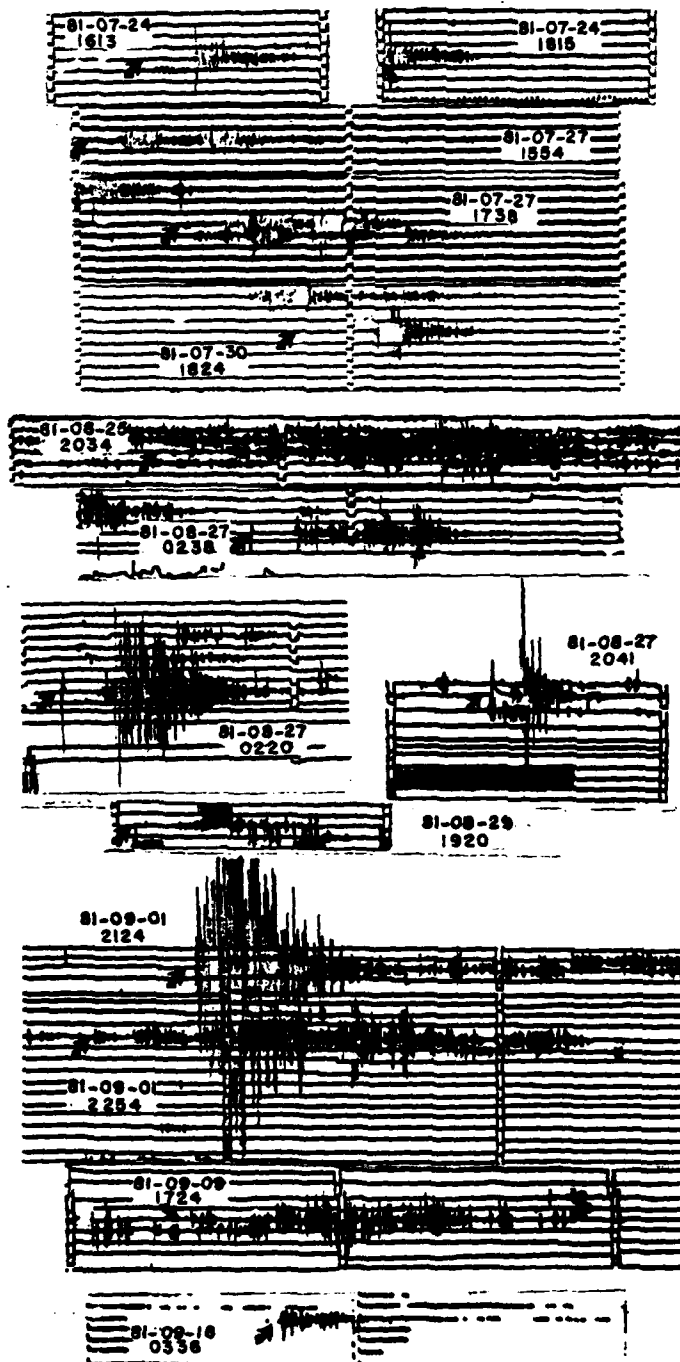


Figure 18. Seismograms from the Capulin seismic survey. The day-time groups correspond to Table 2.

## CHAPTER IV

### CONCLUSIONS

The geophysical measurements and the interpretation reported in this thesis meet the objectives set out in Chapter I. Furthermore, the interpretation of the data of these geophysical surveys lead to the following results:

1. The free air and Bouguer gravity data both indicate the study area is in near perfect isostatic adjustment. Correlation between this report and studies in adjacent areas indicate the Colorado - northeast New Mexico - west Texas region is in isostatic balance.

2. A large free air gravity anomaly in the southern portion of the study area is the result of local crustal loading by Quaternary volcanic activity. The thickness of the volcanic rock is estimated to 180 m based on the gravitational effect represented in the free air anomaly.

3. The basement relief map constructed from Bouguer gravity data has a high correlation with known geologic structures.

4. The Raton magnetic map generally represents the same basement surface as that constructed from Bouguer gravity data.

5. The Capulin area and adjacent High Plains are seismically active. Further investigation of the local seismicity is important.

6. The basement structure map and Raton magnetic map indicate areas of potential benefit in future petroleum exploration. The high heat flow in the Basin may have economic importance. If the heat flow is found to be a result of dormant vulcanism, seismic studies, as in the Capulin area, may be helpful in determining the extent of the thermal field.

References Cited

- Bachman, G.O.; C.H. Dane, 1962, Preliminary Geologic Map of the north-eastern part of New Mexico, USGS Misc. Geologic Investigations, Map I-358.
- Baldwin, B.; W.R. Muehlberger, 1959, Geologic Studies of Union County, N.M., N.M. Bureau of Mines and Mineral Resources (NMBMMR), Bull. 63, Socorro, NM.
- Baltz, E.H., 1965, Stratigraphy and History of Raton Basin and Notes on San Luis Basin, Colorado-New Mexico, AAPG, Bull., V. 49, No. 11, p. 2041-2075.
- Brill, K.G., 1952, Stratigraphy in the Permo-Pennsylvanian zeugogeosyncline of Colorado and northern New Mexico, GSA, Bull., V. 63, No. 8, p. 809-880.
- Clark, S.P., 1966, Handbook of Physical Constants, GSA Memoir 97, p.467-481.
- Compton, R.R., 1962, Manual of Field Geology, John Wiley & Sons, Inc., NY, NY, p. 338.
- Davis, J., 1973, Statistics and Data Analysis in Geology, John Wiley & Sons, Inc., NY, NY.
- Dobrin, M.B., 1976, Introduction to Geophysical Prospecting, 3rd Edition, McGraw-Hill Books, San Francisco, CA.
- Edwards, C.C.; M. Reiter; C. Shearer; W. Young; 1978, Terrestrial heat flow and crustal radioactivity in northeastern New Mexico and southeastern Colorado, GSA, Bull., V. 89, p. 1134-1350.
- Griggs, R.C., 1948, Geology and Ground Water Resources of eastern Colfax County, New Mexico, MNBMMR, Socorro, NM.
- Hamilton, W.; L.C. Pakiser, 1965, Geology and Crustal cross section of the United States along the 37th Parallel, USGS Misc. Geologic Investigations, Map I-448.
- Johnson, R.B., 1969, Geologic Map of the Trinidad Quadrangle South Central Colorado, USGS Misc. Geologic Investigations, Map I-558.

- Jones, L.M.; R.C. Walker; J.C. Stormer, 1974, Isotope composition of Sr and the origin of volcanic rocks of the Raton - Clayton District, northeast New Mexico, GSA, Bull., V. 85, p. 33-36.
- Jurice, C.A.; L.C. Gerhard, 1969, Colorado Raton Basin: mineral resources and geologic section, Mountain Geologist, V. 6, No. 3, p. 81-84.
- McGehee, J.R., 1955, Colorado Measured Section, Rocky Mountain Assoc. of Geologists, Denver, Colorado.
- Qureshy, M.N., 1962, Gravimetric - isostatic studies in Colorado, JGR, V. 67, No. 7, p. 2459-2467.
- Reiter, M.; A.J. Mansure; C. Shearer, 1979, Geothermal characteristics of the Rio Grande rift within the southern Rocky Mountain complex, in, Rio Grande rift: Tectonics and Magmatism (R.E. Riecker, ed.), AGU, Washington, D.C., p. 253-267.
- Reinhart, P.S., 1981, SAS/Graph User's Guide, 1981 Edition, SAS Institute, Inc., Cary, NC.
- Sanford, A.R., 1981, Earthquakes in New Mexico, 1978-1980, (unpublished manuscript).
- \_\_\_\_ K.H. Olsen; L.H. Jaksha, 1981, Earthquakes in New Mexico, 1849-1977, NMBMR, Circular 171.
- Shurbet, D.H., 1966, Gravity field and isostatic equilibrium of the Llano Estacado of Texas and New Mexico, GSA, Bull., v. 77, p. 213-222.
- Smith, R.B., 1970, Regional gravity survey of western and central Montana, AAPG, Bull., V. 67, No. 2, p. 2459-2467.
- Stewart, S.W.; L.C. Pakiser, 1962, Crustal structure in eastern New Mexico interpreted from the Gnome Expedition, SSA, Bull., V. 52, p. 1017-1030.
- Stormer, J.C., 1972, Ages and nature of volcanic activity on the high plains of New Mexico and Colorado, GSA, Bull., V. 83, p. 2443-2448.
- Suppe, J.; C. Powell; R. Berry, 1975, Regional topography, seismicity, Quaternary volcanism, and the present-day tectonics of the western United States, Am. J. of Science, V. 275-A, p. 379-436.
- Wanek, A.A., 1963, Geology and fuel resources of the southwestern part of the Raton Coal Field, Colfax County, New Mexico, USGS Coal Investigations, Map C-45.

Wanek, A.A.; C.B. Read; G.O. Robinson; W.H. Hayes; M. McCallum, 1964, Geologic Map and Sections of Philmont Ranch Region, New Mexico, USGS Misc. Geologic Investigations, Map I-425.

Wollard, G.P., 1959, Crustal structure from gravity and seismic measurements, JGR, V. 64, No. 10, p. 1521-1544.

\_\_\_\_\_ 1962, The relation of gravity anomalies to surface elevation, crustal structure and geology, U. Wisc. Geophysics Polar Res. Center, Report 62-9.

\_\_\_\_\_ 1969, Regional variation in Gravity, in, The Earth's Crust and Upper Mantle (P.J. Hart, ed.), AGU Monograph 13, Washington D.C., p. 320-341.

Zeitz, I.; P.C. Bateman; M.D. Crittenden; A. Giscom; E.R. King; R.J. Roberts; G.R. Lorentzen, 1969, Aeromagnetic investigation of crustal structure for a strip across the western United States, GSA, Bull., V. 80, No. 9, p. 1703-1714.

## APPENDIX A

## NOAA GRAVITY AND ELEVATION DATA

Explanation of Table Headings

Lat Northern latitude of station in degrees.

Long Western longitude of station in degrees.

Elev Station elevation in meters above sea level.

FAA Free air anomaly, calculated from a datum of sea level. The free air correction (FAC) is 0.3085 mgal/m and is applied to the observed gravity reading (OGR):  $FAA = OGR + FAC$ .

BA Bouguer anomaly, calculated using a datum of sea level, station elevation, and a density of 2.67 g/cc. The Bouguer correction (BC) is  $2\pi\gamma h$ , or 0.0837 mgal/m, and is applied to the FAA:  
 $BA = FAA - BC$ .

LAT	LONG	FLY	FAB	FA
37.500	104.247	1728.300	-9.1000	-193.5000
37.275	104.377	1743.300	-13.5000	-208.5000
37.327	104.375	1732.200	-10.3000	-204.1000
37.343	104.638	1765.400	-15.1000	-182.5000
37.117	104.247	1745.000	-2.6000	-192.5000
37.056	104.880	2010.400	-4.0000	-234.5000
37.400	104.638	1938.300	-7.5000	-227.1000
37.403	104.827	1918.400	-7.2000	-221.9000
37.415	104.640	1931.200	-6.8000	-222.9000
37.600	104.500	1900.000	-0.4000	-200.5000
37.284	104.845	2077.200	-3.2000	-235.7000
37.289	104.823	2230.100	-4.8000	-243.5000
37.001	104.703	2211.200	-3.7000	-240.5000
37.011	104.752	2289.000	-4.3000	-246.5000
37.016	104.802	2289.700	-7.7000	-246.5000
37.017	104.747	2218.000	-3.5000	-244.3000
37.029	104.729	2152.500	-2.2000	-234.3000
37.024	104.402	2273.200	-13.0000	-234.6000
37.034	104.802	2280.100	-2.1000	-234.6000
37.037	104.934	2331.400	-23.1000	-235.4000
37.037	104.883	2357.400	-7.0000	-237.0000
37.037	104.501	2114.700	-14.5000	-217.0000
37.153	104.342	1852.000	-18.4000	-225.0000
37.156	104.422	2381.200	-11.4000	-238.0000
37.159	104.637	1983.000	-13.3000	-233.2000
37.160	104.307	2079.900	-13.4000	-246.0000
37.162	104.954	2246.700	-8.1000	-237.5000
37.162	104.503	1836.100	-19.6000	-232.4000
37.162	104.807	2199.700	-13.7000	-224.8000
37.162	104.503	1824.500	-22.0000	-229.7000
37.207	104.833	2033.300	-8.6000	-239.7000
37.217	104.833	2243.000	-4.0000	-244.0000
37.240	104.702	2131.200	-2.2000	-240.0000
37.252	104.654	2328.100	-11.5000	-243.5000
37.187	104.057	2017.500	-10.7000	-238.4000
37.189	104.510	1894.000	-13.7000	-227.5000
37.276	104.687	2136.900	-9.0000	-235.0000
37.297	104.702	2265.000	-18.0000	-233.5000
37.134	104.574	1887.900	-15.5000	-226.5000
37.142	104.837	2134.300	-14.5000	-226.5000
37.152	104.512	1921.800	-4.5000	-223.0000
37.152	104.915	2142.700	-10.8000	-236.2000
37.129	104.803	2047.300	-13.7000	-237.4000
37.129	104.646	2087.300	-13.3000	-237.4000
37.122	104.708	1972.700	-19.7000	-240.4000
37.124	104.648	1938.200	-15.2000	-232.7000
37.128	104.684	1946.600	-18.5000	-233.6000
37.129	104.597	1888.500	-16.4000	-227.0000
37.121	104.729	1979.400	-21.1000	-242.0000
37.110	104.526	1938.000	-2.4000	-231.0000
37.075	104.803	1980.300	-9.0000	-231.4000
37.075	104.657	2115.000	-11.6000	-248.5000
37.077	104.519	2016.900	-6.4000	-219.1000
37.096	104.817	1941.300	-4.1000	-229.4000
37.100	104.790	2058.300	-17.1000	-247.4000
37.051	104.312	2130.700	-3.7000	-249.0000
37.051	104.876	2361.200	-3.3000	-234.0000
37.295	104.511	1824.100	-17.6000	-232.0000
37.295	104.530	1864.800	-10.3000	-224.6000
37.400	104.830	1946.500	-3.1000	-220.0000
37.155	104.914	2192.700	-10.4000	-235.5000
37.127	104.337	2087.300	-17.5000	-250.0000
37.122	104.736	2021.100	-16.9000	-242.5000
37.122	104.847	1949.500	-15.8000	-230.7000
37.142	104.557	1888.200	-15.9000	-224.7000
37.132	104.312	1955.000	-3.5000	-214.5000
37.044	104.506	2109.200	-20.4000	-215.3000
37.170	104.511	1829.100	-19.9000	-224.0000

Copy available to DTIC does not permit fully legible reproduction

LAT	LONG	ELEV	FAA	FA
37.295	104.530	1864.700	-18.500	-227.200
37.400	104.600	1946.400	-5.300	-223.100
37.135	104.610	1901.000	-15.400	-228.100
37.130	104.532	2072.000	-18.400	-250.200
37.173	104.512	1825.800	-20.700	-225.000
37.167	104.508	1826.100	-21.400	-225.000
37.337	104.503	1900.400	-14.400	-227.000
37.410	104.967	2642.000	60.800	-234.700
37.405	104.624	1921.500	-8.400	-223.400
37.447	104.652	1952.200	-4.500	-227.000
37.426	104.587	1887.900	-9.500	-220.700
37.420	104.979	2501.500	+7.000	-238.000
37.442	104.763	2137.000	9.300	-229.700
37.472	104.352	2180.000	13.400	-230.500
37.473	104.818	2159.500	13.000	-228.400
37.475	104.800	2152.700	11.000	-227.000
37.480	104.882	2175.100	12.300	-230.000
37.480	104.752	2103.100	0.400	-220.700
37.482	104.532	1801.500	-4.300	-214.500
37.450	104.535	1933.000	-3.300	-220.100
37.500	104.712	1969.600	-5.700	-226.100
37.408	104.670	1966.000	-6.000	-226.900
37.352	104.679	1984.900	-3.000	-225.900
37.355	104.805	2205.000	0.200	-230.400
37.380	104.938	2367.400	33.000	-231.700
37.309	104.707	2101.000	10.400	-231.500
37.290	104.602	2301.200	19.400	-247.500
37.302	104.552	1902.500	-15.500	-220.500
37.294	104.935	2516.100	32.800	-248.500
37.292	104.898	2395.400	19.000	-243.400
37.357	104.704	2027.500	-1.400	-228.100
37.307	104.557	1872.400	-9.400	-219.000
37.367	104.501	1839.500	-11.700	-217.500
37.015	104.119	1853.200	22.000	-184.400
37.035	104.016	1799.200	18.700	-182.400
37.042	104.045	1705.700	10.200	-182.200
37.043	104.119	1834.300	21.300	-183.700
37.105	104.335	1853.100	0.400	-207.300
37.102	104.106	1805.800	0.800	-187.600
37.172	104.377	1810.000	-3.500	-206.500
37.184	104.143	1633.700	-9.400	-192.200
37.221	104.275	1719.400	-9.500	-198.400
37.222	104.410	1831.200	-9.500	-214.400
37.222	104.459	1733.100	-20.100	-219.700
37.231	104.354	1787.000	-3.700	-205.700
37.234	104.307	1721.000	-3.500	-202.100
37.235	104.297	1764.200	-8.100	-205.500
37.236	104.087	1049.900	1.700	-182.700
37.238	104.490	1809.300	-15.700	-225.400
37.245	104.425	1705.700	-17.900	-215.500
37.250	104.045	1842.000	1.800	-181.800
37.250	104.118	1726.100	5.400	-187.000
37.205	104.227	1571.200	-4.500	-196.500
37.144	104.107	1002.400	-0.000	-194.000
37.187	104.400	1825.100	-5.500	-209.000
37.278	104.174	1000.400	-3.500	-194.500
37.278	104.210	1091.600	-7.200	-196.500
37.279	104.057	1037.100	0.700	-162.500
37.279	104.247	1723.900	-5.700	-198.600
37.252	104.340	1750.000	-0.000	-204.500
37.261	104.400	1749.500	-10.100	-211.900
37.257	104.151	1714.200	-0.100	-191.500
37.137	104.050	1708.100	7.700	-183.200
37.148	104.332	1777.500	-2.100	-200.900
37.125	104.027	1707.600	9.600	-181.500
37.127	104.269	1700.200	2.200	-194.500
37.113	104.247	1733.700	0.500	-192.900
37.075	104.117	1754.100	12.500	-183.000

Copy available to DTIC does not  
 permit fully legible reproduction

LAT	LONG	ELEV	FAA	TA
37.076	104.185	1745.600	7.100	-188.000
37.079	104.182	1783.100	12.700	-189.000
37.108	104.383	2913.500	20.000	-205.100
37.155	104.202	1717.500	3.000	-189.000
37.087	104.050	1748.600	13.500	-181.000
37.092	104.472	2219.900	38.000	-210.000
37.097	104.658	1772.700	13.600	-182.500
37.003	104.406	2429.900	80.700	-111.000
37.071	104.371	2171.400	34.900	-207.900
37.065	104.394	1764.500	13.800	-183.000
37.062	104.202	1822.700	11.800	-192.000
37.413	104.247	1886.800	-13.300	-203.100
37.412	104.115	1647.400	0.600	-183.500
37.021	104.491	180.000	19.200	-215.300
37.292	104.302	1714.800	-14.200	-206.000
37.452	104.200	1691.200	1.200	-187.000
37.425	104.464	1751.900	-3.600	-203.000
37.412	104.226	1679.400	-9.200	-197.400
37.454	104.210	1682.500	-2.000	-190.200
37.454	104.243	1683.000	-7.700	-197.700
37.454	104.281	1713.300	-3.200	-199.900
37.461	104.284	1690.100	0.900	-189.000
37.462	104.429	1789.500	0.700	-199.300
37.479	104.164	1712.400	3.100	-185.300
37.480	104.425	1815.100	-3.200	-203.200
37.433	104.385	1727.600	-7.400	-201.200
37.481	104.294	1718.200	-8.600	-201.100
37.433	104.173	1688.500	1.900	-186.800
37.433	104.464	1773.300	-6.200	-204.600
37.436	104.134	1783.500	0.800	-183.600
37.498	104.092	1736.100	11.300	-182.300
37.498	104.223	1719.400	2.300	-189.400
37.494	104.320	1688.600	-12.700	-201.700
37.418	104.401	1748.000	-3.100	-200.700
37.375	104.173	1653.800	-13.900	-198.900
37.381	104.104	1694.400	2.100	-187.300
37.331	104.136	1633.700	-11.700	-194.300
37.331	104.209	1630.400	-13.000	-201.000
37.331	104.317	1855.700	4.000	-203.700
37.331	104.239	1701.700	-11.200	-201.000
37.396	104.464	1788.600	-9.600	-209.700
37.297	104.370	1734.600	-13.400	-207.300
37.307	104.314	1739.200	-11.800	-205.400
37.242	104.487	1801.400	-13.500	-220.100
37.338	104.232	1716.600	-11.200	-203.200
37.363	104.354	1812.300	-4.600	-207.400
37.367	104.465	1790.800	-14.000	-215.100
37.368	104.067	1677.000	0.300	-179.100
37.366	104.392	1801.700	-8.300	-210.300
37.367	104.426	1790.100	-11.400	-211.700
37.360	104.239	1767.500	-4.700	-202.500
37.336	104.172	1649.600	-14.900	-199.300
37.337	104.467	1787.300	-16.400	-216.400
37.337	104.228	1691.900	-14.200	-203.300
37.346	104.012	1583.000	-1.900	-176.700
37.355	104.042	1627.300	3.300	-178.400
37.310	104.287	1745.600	-9.700	-205.000
37.330	104.037	1505.700	-2.300	-182.000
37.335	104.273	1735.800	-10.100	-204.300
37.291	104.429	1772.400	-17.000	-215.300
37.283	104.374	1743.300	-14.100	-209.300
37.903	104.380	1888.500	3.100	-203.000
37.990	104.399	1704.700	-2.200	-193.500
37.990	104.717	1728.600	-3.200	-198.600
37.997	104.615	1754.400	-7.900	-204.200
37.913	104.610	1671.500	-0.300	-187.300
37.903	104.703	1743.900	4.300	-190.400
37.333	104.327	1671.500	0.200	-199.000

LAT	LONG	ELEV	PA	BA
37.905	104.933	2128.700	36.200	-201.600
37.896	104.748	1728.500	1.500	-191.700
37.847	104.545	1822.700	27.500	-176.200
37.545	104.718	1959.600	1.500	-217.300
37.772	104.610	1762.400	14.700	-182.400
37.772	104.632	1850.700	0.500	-200.000
37.749	104.607	1783.200	17.500	-182.100
37.791	104.629	1818.100	-2.300	-203.700
37.792	104.753	1761.400	2.700	-194.200
37.695	104.607	177.400	13.500	-174.800
37.846	104.531	1831.300	29.800	-174.400
37.646	104.945	1771.100	26.900	-213.900
37.852	104.827	1808.100	1.300	-200.800
37.655	104.527	1811.400	-3.400	-203.000
37.820	104.886	1950.600	1.400	-203.700
37.821	104.802	1884.300	3.700	-207.000
37.821	104.897	1952.000	6.100	-212.100
37.827	104.925	2035.800	13.900	-214.000
37.827	104.741	1727.900	0.0	-193.400
37.804	104.712	1775.700	2.000	-191.100
37.864	104.357	1823.300	1.400	-202.500
37.878	104.569	1737.200	13.800	-180.600
37.887	104.854	1853.300	0.700	-200.000
37.893	104.857	1709.300	3.600	-187.400
37.893	104.827	1867.300	8.600	-200.300
37.893	104.834	1831.400	3.100	-203.000
37.910	104.790	1850.300	3.500	-193.100
37.912	104.827	1813.500	3.400	-199.000
37.920	104.624	1762.000	3.000	-188.300
37.921	104.921	2071.100	30.600	-201.000
37.922	104.764	1801.700	3.600	-195.800
37.927	104.898	1952.400	15.000	-203.400
37.928	104.332	1901.000	9.200	-203.400
37.933	104.385	1810.600	0.400	-202.700
37.934	104.422	1825.300	3.000	-201.200
37.936	104.637	1753.800	4.500	-191.500
37.936	104.675	1763.500	2.900	-194.300
37.936	104.712	1767.500	1.600	-196.000
37.936	104.750	1763.000	-1.100	-193.300
37.937	104.946	2144.600	39.300	-200.300
37.994	104.760	1660.600	-15.800	-201.600
37.997	104.523	1605.700	-5.200	-184.400
37.993	104.552	1632.600	-3.100	-187.700
37.993	104.578	1667.600	-4.300	-190.900
37.972	104.562	1684.300	1.400	-186.900
37.973	104.391	1736.100	1.300	-193.100
37.978	104.777	1701.400	-11.600	-202.200
37.941	104.958	2241.800	46.700	-203.900
37.942	104.613	1707.500	3.400	-190.500
37.942	104.937	2348.500	55.600	-216.000
37.953	104.536	1716.000	2.600	-189.300
37.901	104.794	1767.500	-3.200	-203.000
37.945	104.836	1781.600	-2.800	-202.200
37.975	104.842	1972.700	-3.100	-223.300
37.932	104.853	1948.000	-3.300	-221.200
37.607	104.706	1914.300	1.500	-212.700
37.610	104.577	1891.000	1.100	-210.300
37.547	104.625	1917.200	-4.500	-219.100
37.606	104.587	1896.500	0.500	-211.500
37.596	104.774	1925.600	-3.500	-213.600
37.571	104.590	1903.800	4.700	-214.500
37.500	104.422	2009.900	-3.500	-229.400
37.503	104.740	1934.300	-2.100	-213.400
37.529	104.643	1891.600	-4.800	-221.300
37.542	104.573	1942.500	1.900	-215.300
37.542	104.847	1902.900	-5.700	-217.000
37.542	104.552	2047.000	-3.700	-232.000
37.542	104.536	1965.400	3.200	-214.500

Copy available to DTIC does not  
 permit fully legible reproduction

LAT	LONG	ELEV	FAA	EA
37.523	104.856	2074.200		
37.521	104.872	2119.300	4.500	-227.400
37.521	104.899	1952.900	-3.800	-227.400
37.522	104.977	2032.400	-1.500	-235.100
37.611	104.672	1866.600	-2.300	-235.900
37.610	104.642	1851.200	-1.500	-210.300
37.618	104.608	1880.600	-3.500	-210.400
37.617	104.794	1864.600	-0.400	-210.600
37.622	104.782	1884.300	-3.600	-215.600
37.607	104.751	1875.300	-2.500	-219.300
37.633	104.815	1908.400	-3.400	-210.300
37.632	104.780	1912.600	0.0	-215.300
37.627	104.554	1890.700	1.200	-212.300
37.604	104.705	1830.600	3.300	-208.100
37.614	104.523	1878.500	-2.100	-205.700
37.645	104.873	1910.600	-0.300	-210.400
37.652	104.744	1867.200	1.300	-212.400
37.650	104.910	1814.800	-0.200	-208.600
37.650	104.842	1912.600	-0.400	-205.400
37.650	104.764	1825.400	2.100	-211.700
37.660	104.552	1834.600	0.700	-203.300
37.660	104.873	1802.300	6.300	-203.900
37.672	104.800	1857.800	1.100	-200.400
37.683	104.920	2010.100	-2.900	-210.600
37.683	104.793	1850.800	-2.600	-228.800
37.735	104.743	1727.900	-2.900	-210.700
37.715	104.750	1764.700	1.700	-191.400
37.715	104.955	1959.300	4.800	-192.700
37.717	104.743	1823.600	11.000	-203.100
37.745	104.567	1749.900	6.100	-198.300
37.747	104.707	1702.600	1.200	-194.300
37.725	104.781	1882.400	-13.300	-200.700
37.710	104.818	1872.700	-3.300	-210.700
37.847	104.833	1809.600	4.700	-204.600
37.710	104.818	1872.600	4.800	-197.600
37.847	104.833	1808.900	2.100	-207.300
37.523	104.692	1952.600	12.000	-200.200
37.623	104.781	1852.400	-3.000	-221.300
37.620	104.733	1833.400	-2.700	-213.300
37.750	104.833	1818.400	-12.700	-213.400
37.521	104.695	1917.200	-6.200	-207.700
37.521	104.821	1924.400	-8.800	-223.300
37.510	104.947	1915.100	-7.100	-223.300
37.513	104.907	2181.300	-9.200	-223.300
37.512	104.939	2123.200	12.200	-231.700
37.504	104.630	1939.100	3.300	-234.100
37.508	104.975	2137.300	-5.600	-224.300
37.505	104.535	1942.300	2.000	-230.900
37.505	104.622	1908.700	3.500	-215.700
37.505	104.844	1944.600	10.400	-224.000
37.505	104.862	1987.000	-7.200	-224.800
37.504	104.832	1916.300	-4.400	-224.800
37.504	104.684	1961.100	10.100	-224.500
37.675	104.895	1913.200	-3.600	-225.000
37.674	104.652	1776.700	2.100	-211.600
37.647	104.552	1913.300	1.000	-198.800
37.647	104.857	1938.500	17.100	-198.800
37.637	104.887	1802.400	4.900	-211.600
37.644	104.763	1824.400	4.900	-197.000
37.693	104.827	1765.900	-1.800	-206.400
37.695	104.809	1865.700	-0.300	-194.400
37.695	104.833	1738.200	-3.600	-209.200
37.702	104.710	1797.100	3.200	-211.700
37.705	104.677	1773.300	1.700	-194.100
37.706	104.878	1928.200	4.200	-194.400
37.705	104.585	1798.900	3.400	-212.200
37.712	104.437	1943.400	10.200	-195.400
37.713	104.304	1420.600	0.300	-211.600
			2.500	-212.600

LAT	LONG	ELEV	FAA	EA
37.717	104.552	1829.100	15.400	-189.500
37.717	104.555	1819.500	17.400	-186.000
37.725	104.737	1831.300	0.100	-198.500
37.731	104.809	1798.900	0.800	-184.500
37.731	104.820	1851.400	-0.900	-208.000
37.730	104.802	1800.900	13.200	-189.800
37.748	104.817	1752.000	10.700	-185.100
37.748	104.842	1810.500	13.100	-187.500
37.750	104.629	1720.000	7.900	-184.500
37.755	104.892	1781.900	5.400	-190.800
37.801	104.832	1860.100	-23.800	-185.100
37.775	104.150	1459.400	-23.100	-186.500
37.760	104.302	1507.500	-18.400	-187.100
37.757	104.175	1550.300	-15.400	-188.500
37.818	104.200	1576.400	-9.000	-185.400
37.806	104.275	1632.200	2.100	-180.400
37.945	104.437	1635.000	0.400	-176.400
37.746	104.225	1459.100	-13.800	-177.100
37.950	104.318	1545.300	-4.300	-177.200
37.955	104.217	1375.700	-21.400	-175.500
37.905	104.110	1392.300	-22.700	-178.500
37.992	104.308	1518.500	-5.600	-175.000
37.995	104.267	1440.000	-14.000	-175.900
37.900	104.000	1400.000	-10.000	-170.000
37.918	104.253	1483.500	-12.000	-178.000
37.902	104.495	1697.400	12.800	-176.900
37.905	104.400	1640.300	13.400	-173.700
37.855	104.430	1683.200	14.200	-174.100
37.822	104.058	1423.400	-25.700	-185.000
37.842	104.500	1784.000	24.500	-174.800
37.848	104.250	1502.700	-3.700	-180.500
37.800	104.115	1457.400	-19.500	-180.100
37.837	104.025	1543.200	-17.900	-190.000
37.805	104.065	1504.700	-15.000	-192.500
37.947	104.110	1651.100	-7.200	-191.900
37.858	104.070	1634.500	-15.700	-195.000
37.600	104.187	1777.300	0.200	-198.400
37.475	104.435	1593.500	-3.400	-181.500
37.474	104.213	1441.400	-15.100	-176.400
37.944	104.297	1460.700	-13.000	-177.200
37.965	104.297	1490.000	-10.000	-177.500
37.907	104.127	1432.900	-15.500	-176.000
37.477	104.250	1433.300	-13.900	-176.500
37.435	104.172	1442.500	-15.100	-176.500
37.937	104.132	1435.300	-17.500	-173.100
37.437	104.170	1423.900	-17.500	-177.700
37.950	104.380	1350.200	-2.500	-179.000
37.954	104.041	1408.500	-17.900	-175.500
37.948	104.415	1689.500	9.400	-179.500
37.800	104.157	1480.300	-12.400	-179.500
37.801	104.431	1730.000	10.900	-170.500
37.804	104.267	1515.400	-7.000	-175.700
37.575	104.300	1650.000	-18.100	-202.900
37.577	104.425	1805.900	-3.000	-205.700
37.610	104.454	1814.200	-3.500	-211.800
37.535	104.137	1767.500	4.400	-195.200
37.594	104.043	1560.000	-17.300	-194.400
37.540	104.104	1600.200	-3.700	-191.500
37.554	104.087	1646.500	-7.400	-191.700
37.557	104.190	1758.100	3.500	-193.000
37.566	104.052	1600.000	-11.400	-191.200
37.500	104.051	1692.500	-1.100	-195.400
37.500	104.445	1343.900	-2.400	-209.500
37.539	104.430	1370.000	2.300	-206.500
37.542	104.292	1568.000	-13.800	-199.500
37.522	104.210	1723.500	3.700	-190.000
37.522	104.135	1688.900	1.100	-187.700
37.612	104.025	1555.100	-17.400	-191.800

LAT	LONG	ELEV	FAA	CA
37.015	104.378	1763.900	-7.100	-204.500
37.015	104.313	1673.200	-17.300	-204.700
37.022	104.194	1697.700	-5.400	-195.500
37.013	104.472	1820.300	-8.000	-213.300
37.640	104.018	1542.800	-13.500	-191.100
37.014	104.322	1557.800	-13.100	-204.500
37.014	104.423	1749.800	-16.900	-212.500
37.013	104.334	1700.800	-13.300	-205.700
37.012	104.195	1699.800	-5.300	-195.500
37.031	104.071	1533.800	-17.400	-191.500
37.015	104.169	1592.300	-17.300	-195.500
37.073	104.077	1688.800	-11.500	-195.500
37.073	104.107	1630.400	-10.500	-192.400
37.000	104.147	1622.800	-13.800	-195.400
37.072	104.002	1504.300	-19.100	-187.500
37.039	104.140	1619.100	-13.500	-194.700
37.725	104.250	1644.100	-5.800	-191.500
37.517	104.000	1703.200	-3.100	-185.500
37.312	104.429	1785.800	-8.100	-206.600
37.334	104.334	1711.100	-4.500	-186.700
37.508	104.343	1730.700	-8.800	-202.400
37.302	104.158	1712.100	-8.200	-185.200
37.677	104.367	1713.000	-9.400	-201.100
37.077	104.328	1682.300	-10.200	-199.100
37.087	104.393	1777.800	-3.100	-198.800
37.090	104.082	1672.700	-2.400	-190.100
37.700	104.422	1841.300	10.400	-195.500
37.728	104.452	1853.200	13.800	-138.400
37.729	104.100	1558.700	-14.300	-188.700
37.740	104.448	1809.300	15.200	-184.100
37.748	104.478	1852.000	23.800	-183.200
37.793	104.226	1617.900	-3.000	-184.100
37.796	104.500	1831.300	28.100	-176.700
37.802	104.004	1434.500	-23.100	-185.500
37.803	104.303	1670.300	-6.300	-180.400
37.807	104.127	1452.700	-21.500	-184.000
37.817	104.271	1604.500	-20.100	-179.500
37.773	104.044	1480.200	-20.800	-187.100
37.777	104.337	1827.800	-23.800	-180.500
37.750	104.077	1520.000	-17.500	-187.700
37.751	104.445	1887.000	27.800	-183.100
37.753	104.112	1463.000	-7.400	-188.000
37.768	104.500	1843.700	25.800	-180.200
37.773	104.408	1851.700	25.800	-181.400
37.784	104.137	1463.000	-22.300	-186.000
37.792	104.332	1753.200	17.300	-178.500
37.849	104.497	1811.400	24.300	-173.200
37.850	104.199	1508.500	-12.700	-181.500
37.850	104.464	1779.100	23.300	-175.100
37.830	104.142	1487.400	-13.700	-182.100
37.819	104.497	1823.200	19.000	-175.400
37.828	104.241	1564.500	-4.500	-179.500
37.865	104.146	1464.600	-14.900	-178.800
37.872	104.114	1434.900	-17.200	-178.500
37.889	104.077	1424.000	-17.900	-177.200
37.889	104.400	1753.800	10.800	-179.200
37.890	104.040	1410.800	-16.300	-174.100
37.903	104.113	1438.200	-13.400	-176.500
37.910	104.003	1394.500	-16.500	-172.500
37.910	104.252	1485.500	-11.500	-177.500
37.923	104.132	1421.300	-13.100	-177.200
37.923	104.041	1407.000	-13.900	-173.400
37.933	104.077	1426.300	-15.300	-175.200
37.931	104.268	1499.900	-10.300	-173.100
36.000	104.010	1719.800	44.100	-148.300
35.072	104.488	1824.500	24.600	-179.500
35.100	104.485	1804.700	8.800	-193.100
35.305	104.050	1551.900	49.100	-158.100

FAI	LUSG	FLYV	FAA	SA
35.307	104.295	1857.500	39.500	-159.400
35.320	104.402	1817.100	21.000	-182.200
35.407	104.402	1842.000	24.500	-181.500
35.437	104.438	1759.500	7.900	-193.500
35.023	104.154	1821.900	40.000	-157.700
35.040	104.235	1850.700	42.100	-164.700
35.007	104.028	1751.500	46.800	-149.000
35.055	104.325	1768.500	40.500	-157.200
35.074	104.133	1800.500	49.800	-151.400
35.177	104.397	1771.300	13.900	-184.500
35.142	104.064	1779.900	49.300	-149.700
35.247	104.412	1771.000	15.400	-182.600
35.191	104.330	1758.300	21.900	-174.500
35.490	104.355	1418.400	17.500	-197.200
35.435	104.285	2033.500	36.500	-190.700
35.400	104.300	1375.100	23.400	-180.200
35.436	104.295	1919.300	26.600	-187.700
35.370	104.302	1805.700	50.000	-178.900
35.305	104.008	1808.500	46.400	-155.700
35.305	104.101	1377.500	42.700	-157.100
35.306	104.350	1810.300	23.400	-174.500
35.250	104.353	1820.900	43.400	-160.100
35.277	104.321	1844.000	37.400	-165.800
35.357	104.259	1762.800	49.400	-170.000
35.114	104.354	1795.300	33.700	-167.000
35.031	104.072	1746.500	43.100	-152.300
35.126	104.361	1895.800	46.500	-165.500
35.370	104.244	1937.100	51.000	-171.100
35.407	104.152	1950.200	50.400	-167.000
35.425	104.055	1905.300	41.300	-171.700
35.437	104.242	2015.700	42.400	-182.900
35.450	104.127	2300.800	75.500	-181.400
35.152	104.133	1861.200	62.300	-145.700
35.148	104.205	1379.500	50.900	-159.200
35.303	104.167	1744.500	33.200	-164.200
35.304	104.095	1705.200	50.000	-162.400
35.227	104.152	1857.100	55.400	-155.400
35.276	104.259	1800.200	45.500	-162.200
35.307	104.098	1808.500	50.400	-150.500
35.305	104.183	1723.000	54.500	-161.100
35.216	104.072	1873.300	56.400	-153.000
35.172	104.250	1800.500	54.000	-165.000
35.307	104.025	1808.700	45.900	-158.500
35.308	104.260	1677.300	40.200	-169.000
35.912	104.444	2046.700	24.400	-204.300
35.440	104.432	2373.000	50.200	-215.000
35.692	104.437	2017.200	21.100	-204.300
35.811	104.410	1937.000	9.700	-206.700
35.748	104.462	1888.400	5.100	-205.900
35.540	104.303	1937.500	18.400	-197.500
35.655	104.443	1981.600	20.700	-200.900
35.657	104.325	2042.000	30.100	-195.400
35.703	104.387	1906.200	4.900	-208.300
35.305	104.457	1970.000	15.000	-205.500
35.912	104.444	2046.700	22.000	-206.800
35.705	104.442	1926.500	7.500	-205.500
35.840	104.223	2072.300	36.600	-195.000
35.538	104.140	2193.500	32.500	-192.700
35.877	104.026	2008.700	47.100	-186.400
35.901	104.115	2049.500	72.500	-190.200
35.053	104.328	2052.400	31.700	-197.800
35.025	104.143	2200.000	53.000	-195.000
35.995	104.325	2034.400	64.600	-210.000
35.990	104.154	1951.500	32.100	-130.000
35.915	104.205	2434.300	80.500	-194.000
35.952	104.260	2476.500	76.400	-190.500
35.909	104.039	1935.000	52.400	-184.000
35.910	104.327	2515.400	95.300	-202.100

Copy available to DTIC does not  
 permit fully legible reproduction



LAI	LENO	ELEV	FAA	SA
36.405	104.820	2156.500	19.700	-221.400
36.807	104.471	2382.500	27.300	-235.800
36.829	104.888	1921.400	21.300	-193.500
36.512	104.774	1900.400	-3.400	-213.500
36.623	104.756	1907.100	19.100	-194.100
36.825	104.823	1987.300	23.400	-198.300
36.614	104.943	2146.300	26.400	-213.700
36.894	104.987	2323.000	38.800	-221.100
36.587	104.851	1970.200	15.300	-205.500
36.557	104.538	1799.200	3.400	-197.700
36.655	104.533	1807.200	7.300	-201.500
36.311	104.427	1964.600	10.100	-210.100
36.514	104.940	1991.000	4.900	-212.700
36.518	104.904	2008.000	9.200	-215.500
36.523	104.947	2039.400	0.400	-221.000
36.587	104.926	2164.200	33.500	-210.500
36.117	104.560	1916.300	12.000	-201.000
36.117	104.600	1903.000	7.000	-203.400
36.117	104.668	1902.400	7.400	-203.300
36.119	104.923	2191.200	35.800	-204.200
36.114	104.481	2254.000	31.200	-220.900
36.115	104.512	2018.700	0.700	-190.600
36.113	104.771	2021.400	25.500	-202.500
36.302	104.543	1783.200	4.800	-194.300
36.007	104.700	1889.500	1.100	-210.200
36.193	104.660	1823.400	4.400	-194.200
36.888	104.885	1909.000	4.000	-209.400
36.095	104.737	1904.300	4.700	-208.500
36.113	104.590	2150.300	35.500	-203.000
36.108	104.541	1903.400	12.500	-200.700
36.177	104.498	2169.900	19.400	-223.300
36.203	104.835	1953.000	12.100	-208.400
36.205	104.695	1833.000	4.900	-200.700
36.235	104.580	1843.400	5.500	-200.500
36.313	104.805	2128.000	51.700	-197.000
36.323	104.920	2016.100	15.900	-208.000
36.363	104.717	1829.500	5.400	-194.200
36.405	104.617	1839.200	4.500	-201.200
36.415	104.858	1913.400	7.500	-208.000
36.477	104.757	1874.000	-7.500	-217.500
36.024	104.537	1387.300	23.500	-187.500
36.026	104.095	1060.000	1.400	-208.700
36.397	104.937	2050.700	22.100	-207.200
36.408	104.860	1923.000	5.500	-209.500
36.460	104.950	2018.100	10.100	-209.500
36.530	104.923	1990.500	14.000	-207.400
36.303	104.397	1940.100	12.800	-204.100
36.294	104.927	2071.700	20.300	-211.300
36.117	104.680	1913.500	8.200	-205.700
36.117	104.590	1894.500	7.500	-204.500
36.435	104.843	1902.300	8.000	-204.100
36.436	104.792	1882.600	0.200	-210.200
36.480	104.770	1873.900	-0.100	-215.700
36.303	104.697	2160.000	46.700	-208.700
36.262	104.837	1913.100	13.400	-200.700
36.261	104.703	1834.400	10.700	-200.100
36.348	104.792	1888.500	15.500	-193.000
36.035	104.050	1947.100	10.400	-207.200
36.079	104.730	1932.400	3.900	-207.100
36.071	104.943	2190.000	25.700	-219.100
36.068	104.542	1917.200	10.800	-203.500
36.050	104.527	1870.000	17.300	-191.800
36.044	104.532	1928.500	4.000	-206.000
36.050	104.781	2001.400	17.200	-208.000
36.020	104.810	1995.300	13.000	-203.200
36.022	104.752	1905.000	11.300	-208.200
36.013	104.543	1901.300	23.900	-188.000
36.013	104.050	1928.500	8.500	-207.100

Copy available to DTIC does not permit fully legible reproduction

14T	LOVE	FLY	FAA	BA
30.0000	103.014	1944.000	13.400	-203.900
30.0000	103.044	2148.800	17.800	-212.600
30.0000	103.074	1953.200	9.900	-208.500
30.0000	103.104	2059.200	37.400	-205.000
30.0000	103.134	2155.200	32.000	-201.700
30.0000	103.164	2135.000	30.900	-207.000
30.0000	103.194	1478.600	-1.100	-106.500
30.0000	103.224	1410.700	-11.100	-109.700
30.0000	103.254	1407.000	5.900	-151.500
30.0000	103.284	1725.900	27.800	-104.000
30.0000	103.314	1585.900	12.000	-105.300
30.0000	103.344	1621.700	20.000	-164.700
30.0000	103.374	1608.400	15.300	-164.500
30.0000	103.404	1600.500	15.400	-165.100
30.0000	103.434	1514.900	1.800	-168.100
30.0000	103.464	1561.200	14.800	-154.700
30.0000	103.494	1585.000	18.400	-158.700
30.0000	103.524	1481.000	5.200	-100.400
30.0000	103.554	1521.000	11.700	-150.400
30.0000	103.584	1405.800	1.000	-100.000
30.0000	103.614	1407.000	4.200	-150.800
30.0000	103.644	1611.000	17.700	-162.200
30.0000	103.674	1550.300	6.100	-163.700
30.0000	103.704	1575.300	3.300	-167.500
30.0000	103.734	1483.800	20.800	-139.100
30.0000	103.764	1402.100	11.500	-152.100
30.0000	103.794	1474.000	10.700	-148.000
30.0000	103.824	1500.500	21.700	-145.000
30.0000	103.854	1637.100	15.100	-167.500
30.0000	103.884	1584.400	7.700	-109.400
30.0000	103.914	1414.000	-1.500	-134.400
30.0000	103.944	1408.000	-1.100	-150.500
30.0000	103.974	1348.500	-4.700	-161.000
30.0000	104.004	1383.900	-4.100	-150.200
30.0000	104.034	1374.500	-3.700	-157.200
30.0000	104.064	1381.200	-2.000	-150.400
30.0000	104.094	1367.200	-9.500	-102.100
30.0000	104.124	1433.400	4.200	-150.000
30.0000	104.154	1439.500	5.400	-155.400
30.0000	104.184	1425.900	2.900	-157.000
30.0000	104.214	1426.800	1.000	-157.000
30.0000	104.244	1335.500	7.100	-164.500
30.0000	104.274	1507.100	3.800	-164.600
30.0000	104.304	1434.700	-0.100	-160.700
30.0000	104.334	1459.100	2.300	-160.700
30.0000	104.364	1425.000	2.400	-103.000
30.0000	104.394	1425.000	0.0	-150.500
30.0000	104.424	1478.000	0.300	-104.900
30.0000	104.454	1459.400	1.300	-161.900
30.0000	104.484	1437.700	2.100	-158.500
30.0000	104.514	1478.100	0.100	-165.100
30.0000	104.544	1349.000	-7.500	-104.000
30.0000	104.574	1440.000	-1.500	-163.400
30.0000	104.604	1413.400	-5.100	-163.400
30.0000	104.634	1477.200	0.0	-165.500
30.0000	104.664	1400.000	-7.800	-104.500
30.0000	104.694	1382.300	-7.200	-161.900
30.0000	104.724	1433.500	-7.500	-103.000
30.0000	104.754	1412.100	-7.800	-103.300
30.0000	104.784	1337.400	-4.300	-159.200
30.0000	104.814	1405.100	-6.800	-164.100
30.0000	104.844	1307.500	-8.500	-161.000
30.0000	104.874	1301.200	12.000	-167.900
30.0000	104.904	1040.400	21.500	-162.400
30.0000	104.934	1525.700	1.900	-108.000
30.0000	104.964	1041.700	23.500	-100.000
30.0000	104.994	1421.700	-4.400	-163.500
30.0143	105.027	1590.100	10.500	-160.500

LAT	LONG	ELEV	FAA	HA
36.087	103.132	1387.000	-7.800	-163.100
36.095	103.469	1584.000	25.100	-160.000
36.452	103.189	1334.200	8.000	-164.000
36.410	103.119	1481.400	3.000	-162.000
36.351	103.149	1463.300	3.200	-163.400
36.217	103.130	1441.000	-7.700	-169.000
36.013	103.132	1375.900	-7.700	-161.600
36.079	103.237	1346.000	0.100	-156.000
36.442	103.150	1515.500	5.600	-163.800
36.452	103.187	1341.700	3.000	-160.000
36.148	103.843	1759.000	52.300	-144.400
36.159	103.970	1384.900	37.500	-153.200
36.003	103.824	1656.900	43.300	-139.900
36.117	103.615	1533.000	27.500	-144.300
36.316	103.694	1799.800	44.400	-156.000
36.305	103.794	1751.400	37.700	-150.100
36.252	103.757	1730.700	42.100	-151.300
36.405	103.727	1350.100	33.500	-151.500
36.394	103.649	1793.800	43.200	-133.400
36.321	103.511	1782.300	33.900	-159.400
36.320	103.652	1775.200	42.000	-136.500
36.424	103.840	1895.200	39.700	-132.100
36.412	103.954	1367.500	34.000	-153.000
36.423	103.523	1720.900	29.900	-163.200
36.451	103.900	1914.100	33.300	-160.700
36.257	103.499	1911.100	58.000	-155.700
36.202	103.614	1716.300	38.000	-133.500
36.203	103.852	1724.300	40.500	-146.000
36.175	103.000	1629.200	33.100	-149.000
36.139	103.757	1713.500	49.000	-142.500
36.049	103.592	1462.600	23.800	-139.700
36.051	103.782	1595.400	47.400	-142.100
36.000	103.700	1414.300	21.400	-136.700
36.101	103.400	1713.300	47.300	-144.200
36.112	103.739	1639.300	41.000	-142.200
36.303	103.873	1770.900	40.200	-153.200
36.303	103.747	1743.600	36.100	-158.900
36.322	103.250	1588.900	33.700	-160.100
36.055	103.648	1827.000	25.000	-179.200
36.037	103.084	1590.100	43.100	-106.200
36.627	103.522	1773.900	33.200	-165.100
36.025	103.937	2063.000	47.300	-182.500
36.590	103.610	1810.300	41.300	-161.000
36.590	103.793	1757.100	43.800	-173.000
36.343	103.993	2001.500	56.500	-174.000
36.552	103.703	1880.100	40.700	-183.500
36.510	103.757	1884.500	53.700	-157.000
36.542	103.350	1932.300	43.200	-170.900
36.502	103.545	1756.200	30.400	-166.100
36.394	103.082	1817.000	26.000	-171.200
36.739	103.995	2094.000	43.800	-188.500
36.746	103.755	1930.300	43.400	-172.500
36.705	103.876	2656.900	95.500	-201.700
36.072	103.732	1922.000	42.800	-175.500
36.751	103.538	1770.100	29.000	-168.900
36.397	103.801	1870.900	41.200	-181.000
36.992	103.597	1782.300	23.000	-176.200
36.400	103.975	2073.500	48.000	-183.000
36.932	103.707	1849.400	26.500	-180.300
36.647	103.879	1953.000	33.400	-180.000
36.876	103.560	1813.000	23.000	-177.000
36.244	103.921	1922.700	36.700	-161.700
36.883	103.837	2144.200	37.900	-161.000
36.803	103.064	2030.400	48.000	-179.100
36.815	103.623	1947.600	37.300	-169.300
36.837	103.722	1924.400	37.900	-177.300
36.930	103.752	1943.400	43.000	-173.500
36.742	103.992	2081.200	43.000	-189.000

Copy available to DTIC does not permit fully legible reproduction

AT	LN	FLY	FAA	A
35.593	103.013	1814.500	39.700	-103.100
35.750	103.019	2022.100	40.300	-177.800
35.805	103.958	2101.700	49.000	-100.000
35.979	103.933	2294.200	60.100	-188.400
35.507	103.995	1994.000	40.300	-170.000
35.700	103.022	1428.000	7.000	-152.000
35.449	103.000	1349.400	-3.000	-155.000
35.555	103.142	1404.500	-7.400	-163.100
35.844	103.327	1632.300	10.600	-171.500
35.913	103.227	1497.500	-0.500	-167.500
35.913	103.365	1488.200	-5.300	-171.800
35.712	103.234	1392.500	14.300	-154.200
35.714	103.034	1474.400	0.500	-153.300
35.733	103.414	1586.700	2.200	-173.100
35.533	103.360	1653.600	19.100	-165.700
35.507	103.444	1723.300	20.300	-166.400
35.757	103.307	1628.000	10.400	-162.000
35.735	103.385	1602.000	13.600	-172.400
35.836	103.017	1431.900	-1.000	-161.500
35.795	103.197	1600.800	12.000	-160.400
35.948	103.408	1537.000	-2.100	-174.100
35.717	103.390	1304.200	-3.200	-160.700
35.964	103.195	1404.500	-7.700	-164.300
35.974	103.345	1481.100	-3.000	-168.700
35.750	103.138	1325.600	7.900	-162.700
35.504	103.279	1340.800	1.000	-162.500
35.534	103.121	1477.600	6.500	-158.300
35.034	103.324	1625.700	20.500	-163.200
35.050	103.669	1741.100	20.900	-167.700
35.050	103.101	1555.300	20.000	-151.700
35.612	103.072	1489.000	18.500	-147.900
35.517	103.427	1741.900	28.300	-160.200
35.828	103.443	1716.200	19.900	-172.000
37.732	103.308	1258.200	-14.500	-133.300
37.777	103.250	1262.900	-9.400	-152.900
37.742	103.347	1314.000	-12.000	-160.800
37.996	103.133	1217.400	-20.000	-150.200
37.731	103.390	1205.500	-8.000	-150.200
37.830	103.200	1264.000	-12.400	-133.800
37.777	103.168	1275.000	2.700	-139.900
37.077	103.093	1325.300	-2.300	-150.000
37.440	103.203	1323.900	-21.900	-154.100
37.940	103.133	1217.400	-19.900	-150.200
37.940	103.057	1210.300	-13.200	-149.400
37.939	103.055	1236.600	-13.200	-151.000
37.939	103.200	1292.400	-13.500	-158.100
37.881	103.093	1265.500	-8.500	-150.100
37.350	103.200	1264.000	-12.300	-153.700
37.823	103.142	1280.500	0.0	-143.100
37.778	103.160	1275.000	2.700	-139.900
37.748	103.148	1287.500	-0.100	-144.000
37.748	103.060	1336.700	0.200	-143.400
37.090	103.120	1313.400	-3.800	-150.800
37.091	103.042	1355.400	1.500	-150.000
37.077	103.043	1325.300	-2.400	-150.000
37.054	103.040	1377.700	0.700	-147.300
37.011	103.025	1414.300	4.800	-140.500
37.530	103.002	1444.500	0.000	-150.000
37.529	103.065	1465.900	8.800	-157.300
37.533	103.067	1400.400	7.500	-152.700
37.782	103.137	1289.000	0.400	-137.700
37.800	103.025	1290.800	14.100	-130.100
37.848	103.225	1274.000	-10.600	-153.100
37.033	103.067	1275.500	-0.400	-143.000
37.750	103.267	1314.900	-13.600	-157.800
37.700	103.000	1332.400	2.200	-148.000
37.988	103.398	1258.800	-13.400	-150.200
37.995	103.233	1205.700	-21.300	-150.500

Copy available to DTIC does not  
 permit fully legible reproduction

LAG	LRNG	FLY	FAA	FA
37.507	103.243	1561.800	19.700	-154.700
37.000	103.010	1423.700	9.800	-149.500
37.023	103.000	1375.000	8.000	-145.000
37.042	103.397	1363.700	-0.500	-153.000
37.043	103.057	1342.300	0.500	-149.500
37.505	103.005	1446.400	4.000	-157.300
37.510	103.125	1474.500	4.600	-153.200
37.515	103.353	1330.700	21.100	-154.800
37.533	103.027	1463.600	7.100	-156.400
37.843	103.147	1375.900	-2.200	-155.700
37.845	103.028	1339.000	0.000	-144.100
37.848	103.350	1361.800	0.500	-160.000
37.858	103.070	1422.500	3.000	-150.000
37.555	103.367	1426.200	0.100	-154.200
37.557	103.497	1496.500	0.100	-167.100
37.365	103.363	1588.000	20.400	-157.200
37.146	103.093	1524.300	13.000	-156.900
37.470	103.076	1510.500	13.000	-153.200
37.365	103.083	1588.000	20.400	-157.100
37.270	103.012	1558.700	10.100	-158.100
37.191	103.067	1527.000	16.100	-154.500
37.190	103.012	1550.700	13.600	-156.800
37.146	103.083	1524.300	13.500	-154.000
37.096	103.017	1411.500	3.700	-154.400
37.408	103.067	1550.800	19.600	-159.500
37.265	103.075	1592.800	18.600	-157.500
37.118	103.077	1434.600	29.500	-163.000
37.276	103.342	1721.500	29.400	-159.200
37.337	103.033	1559.400	15.100	-154.200
37.337	103.142	1581.800	21.100	-159.700
37.370	103.083	1589.800	19.000	-157.000
37.382	103.242	1536.800	14.800	-161.800
37.382	103.402	1615.100	18.700	-157.200
37.475	103.073	1434.100	0.900	-156.400
37.475	103.073	1522.200	13.200	-154.400
37.475	103.155	1589.700	9.300	-153.000
37.425	103.167	1505.400	10.300	-160.000
37.472	103.262	1577.600	10.500	-160.000
37.252	103.000	1555.100	19.200	-159.200
37.255	103.290	1668.000	22.800	-169.500
37.255	103.400	1738.500	24.300	-170.000
37.250	103.067	1592.500	14.300	-158.700
37.278	103.083	1593.800	13.100	-160.000
37.173	103.153	1642.000	23.300	-160.500
37.160	103.033	1488.900	10.100	-150.300
37.233	103.083	1505.000	17.500	-159.700
37.233	103.188	1607.200	19.000	-160.000
37.233	103.307	1730.700	23.500	-169.300
37.222	103.498	1786.100	26.700	-173.000
37.142	103.160	1566.100	26.700	-159.100
37.142	103.083	1475.200	10.400	-154.200
37.130	103.003	1400.700	5.700	-150.400
37.130	103.283	1633.700	17.400	-156.200
37.073	103.033	1389.000	-1.000	-156.500
37.000	103.000	1359.400	-3.500	-155.000
37.310	103.212	1718.500	13.400	-173.700
37.599	103.908	1548.400	-0.400	-174.100
37.477	103.520	1690.200	27.400	-161.700
37.143	103.820	1759.900	20.900	-170.400
37.013	103.375	1919.800	35.600	-181.000
37.985	103.533	1239.000	-30.400	-164.100
37.890	103.458	1463.300	-20.000	-183.300
37.988	103.545	1237.900	-31.100	-169.700
37.030	103.710	1417.100	-6.500	-167.500
37.635	103.830	1552.000	-0.200	-173.800
37.543	103.427	1510.500	-7.500	-185.100
37.043	103.965	1324.600	-14.500	-184.900
37.550	103.632	1350.000	-7.100	-175.000

Copy available to DTIC does not permit further distribution

LAT	LONG	ELEV	FAA	EA
37.730	103.540	1356.700	-10.000	-161.500
37.730	103.765	1460.900	-19.300	-172.700
37.735	103.828	1414.600	-23.000	-181.300
37.706	103.908	1431.300	-22.100	-182.200
37.880	103.783	1333.500	-23.500	-172.700
37.927	103.950	1385.000	-15.700	-170.000
37.935	103.937	1357.000	-15.700	-167.600
37.805	103.901	1373.400	-13.100	-165.800
37.863	103.687	1332.600	-22.900	-172.000
37.805	103.965	1414.300	-13.100	-171.300
37.947	103.785	1311.900	-22.200	-169.000
37.932	103.908	1351.300	-18.000	-169.800
37.935	103.675	1306.100	-30.900	-177.100
37.935	103.578	1255.000	-27.900	-171.700
37.990	103.857	1344.800	-18.200	-168.700
37.810	103.767	1349.300	-23.000	-174.000
37.823	103.985	1402.700	-23.900	-160.000
37.817	103.913	1378.000	-12.600	-177.000
37.853	103.597	1341.400	-14.200	-164.300
37.795	103.802	1378.500	-20.800	-175.000
37.995	103.617	1264.300	-33.700	-173.200
37.925	103.725	1310.900	-28.200	-172.900
37.948	103.935	1369.200	-21.400	-174.000
37.600	103.233	1413.700	3.300	-140.700
37.732	103.393	1333.500	-13.000	-162.200
37.735	103.142	1295.000	-2.500	-146.300
37.750	103.165	1256.300	1.800	-141.900
37.755	103.015	1270.500	2.300	-140.500
37.692	103.117	1316.100	-3.500	-150.000
37.847	103.243	1324.700	-10.400	-158.600
37.730	103.415	1296.000	-15.700	-160.300
37.887	103.450	1335.900	-10.600	-160.000
37.870	103.350	1285.200	-14.900	-156.400
37.872	103.025	1250.500	-2.700	-140.500
37.875	103.170	1248.500	-11.700	-151.400
37.885	103.000	1245.100	-1.000	-140.500
37.807	103.190	1245.400	-10.000	-149.300
37.607	103.253	1286.400	-12.000	-153.700
37.935	103.150	1226.900	-19.500	-156.800
37.933	103.465	1287.500	-19.500	-160.500
37.935	103.022	1206.700	-12.800	-147.800
37.935	103.345	1257.600	-14.600	-155.400
37.440	103.245	1246.900	-16.100	-155.700
37.775	103.065	1301.200	-11.000	-134.400
37.775	103.433	1285.600	-17.500	-161.300
37.777	103.157	1305.500	7.800	-138.100

Copy available to DTIC does not  
 permit fully legible reproduction

## APPENDIX B

## CAPULIN GRAVITY AND MAGNETIC DATA

Explanation of Table Headings

Station	Numerical listing of gravity and magnetic station identification. Stations with apostrophe (') are additional magnetic stations.
Lat	Northern latitude of station in degrees.
Long	Western longitude of station in degrees.
Free Air An.	Free air anomaly (FAA) calculated from a datum of sea level. The free air correction (FAC) is 0.3085 mgal/m and is applied to the observed gravity reading (OGR): $FAA = OGR + FAC.$
Bouguer An.	Bouguer anomaly calculated using a datum of sea level, station elevation, and a density of 2.67 g/cc. The Bouguer correction (BC) is $2\pi\gamma h$ , or 0.0837 mgal/m and is applied to the FAA: $BA = FAA - BC.$
Rel. Mag.	Relative vertical magnetic reading in gammas. Datum is station one.

Station	Lat	Long	Free Air An.	Bouguer An.	Rel. Mag.
1	36.805	103.956	49.0	-186.2	0
2	36.806	103.951	48.8	-183.1	695
2'	36.804	103.960			1710
3	36.800	103.965	57.89	-184.5	1395
3'	36.796	103.963			2070
4	36.792	103.963	64.0	-179.5	925
4'	36.790	103.965			850
5	36.794	103.961	59.25	-185.8	1340
5'	36.792	103.966			1790
6	36.790	103.978	60.0	-187.1	1950
7	36.796	103.982	58.5	-186.6	275
7'	36.798	103.979			-1200
8	36.809	103.980	53.0	-183.5	750
9	36.785	103.983	57.85	-189.3	75
10	36.782	103.969	57.06	-188.7	145
11	36.776	103.973	54.4	-187.9	600
12	36.767	103.969	50.6	-186.7	275
12'	36.755	103.978			-150
13	36.759	103.979	49.3	-186.6	200
14	36.752	103.978	54.8	-181.1	450
15	36.743	103.978	47.63	-186.3	1125
16	36.743	103.992	47.8	-186.2	1500
17	36.744	103.984	47.7	-186.2	2425
17'	36.735	103.979			1250
18	36.744	103.973	47.9	-186.1	2125
19	36.746	103.962	47.5	-184.5	2350
20	36.746	103.951	49.05	-182.6	2775
21	36.748	103.938	49.1	-181.6	3625
22	36.748	103.927	50.05	-181.2	3525
23	36.749	103.917	49.9	-181.3	3500
24	36.779	103.979	58.45	-189.4	1375
25	36.784	103.964	59.3	-204.2	3500
26	36.783	103.971	74.6	-195.0	3800
27	36.756	103.917	49.85	-180.2	4650
28	36.759	103.927	48.7	-180.6	4600
28'	36.762	103.926			4525
29	36.764	103.927	49.1	-180.5	4500
30	36.764	103.917	49.5	-179.7	4750
30'	36.761	103.917			5000
31	36.769	103.917	48.1	-179.3	4700
32	36.742	103.936	49.9	-184.2	4920
33	36.734	103.936	52.5	-182.5	3750
34	36.727	103.935	52.3	-183.2	6050
35	36.723	103.935	51.6	-184.5	5500
36	36.716	103.935	51.3	-185.5	3650
37	36.713	103.935	50.85	-185.7	3860
38	36.713	103.944	50.3	-184.7	3950
39	36.713	103.950	48.8	-185.0	4600

Station	Lat	Long	Free Air An.	Bouguer An.	Rel. Mag.
40	36.705	103.953	48.0	-185.4	3300
41	36.698	103.952	47.75	-185.0	3600
42	36.698	103.945	47.8	-185.4	4000
43	36.698	103.934	49.3	-185.1	3600
44	36.741	103.968	49.1	-184.5	3450
45	36.741	103.958	48.9	-183.3	3600
46	36.732	103.958	48.0	-184.5	2450
47	36.727	103.953	48.0	-184.4	3750
48	36.719	103.953	48.4	-184.7	3500
49	36.689	103.965	48.4	-185.3	2850
50	36.689	103.972	48.6	-185.6	3200
51	36.689	103.988	48.2	-186.4	2700
52	36.689	104.023	48.1	-187.7	2000
53	36.689	103.999	48.3	-186.5	2350
54	36.712	103.998	52.1	-186.3	1750
55	36.721	103.998	49.3	-187.7	2000
56	36.727	103.999	48.5	-186.9	1650
57	36.734	103.998	47.9	-188.6	1900
58	36.739	103.996	47.8	-187.3	1900
60	36.743	104.003	47.3	-186.1	1375
61	36.743	104.011	45.9	-186.9	1700
62	36.743	104.021	45.85	-187.7	1275
63	36.746	104.042	44.85	-188.3	1375
64	36.727	104.007	47.7	-186.7	1225
65	36.726	104.016	46.3	-187.5	1400
66	36.726	104.025	47.7	-187.5	1725
67	36.708	104.025	45.7	-188.9	1425
68	36.708	104.036	46.8	-189.8	1325
69	36.787	104.005	52.2	-188.2	1775
70	36.784	104.000	52.55	-187.6	1375
71	36.781	104.001	51.4	-188.1	1500
72	36.828	103.990	53.9	-189.8	1725
73	36.789	103.958	54.4	-187.2	5075
74	36.777	103.962	54.4	-186.0	4000
75	36.777	103.974	57.9	-188.3	2675
76	36.792	103.966	54.4	-185.7	2125
77	36.786	103.960	68.1	-180.6	3900
78	36.789	103.964	58.1	-188.8	2975
79	36.815	103.945	49.5	-178.4	2250

## APPENDIX C

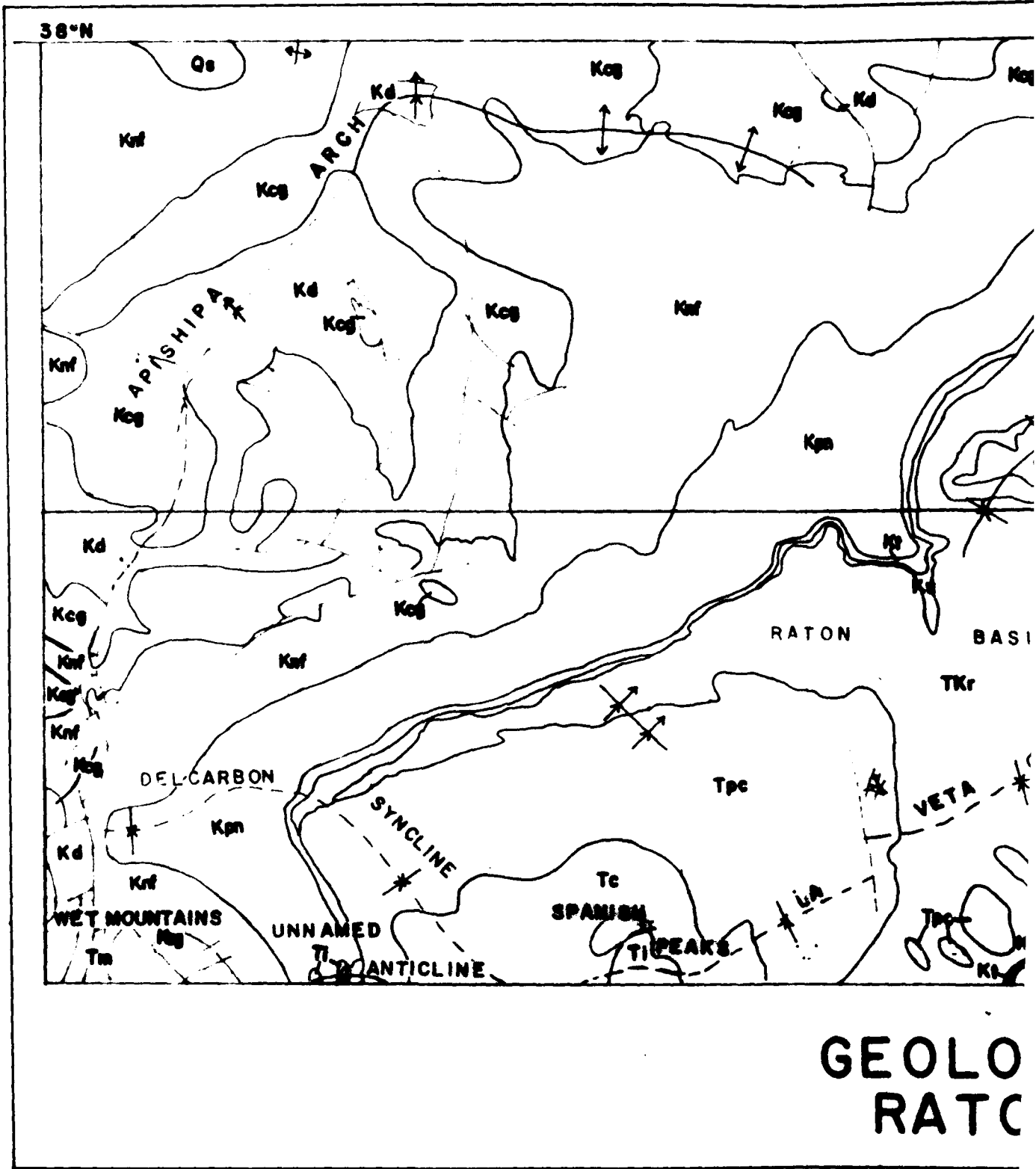
## RATON BASIN MAGNETIC DATA

Explanation of Table Headings

Lat	Northern latitude of station in degrees.
Long	Western longitude of station in degrees.
MAG	Relative vertical magnetic reading in gammas. Station one is datum.

131	132	133	134	135	136
30.348	103.170	53.850	30.341	103.140	502.000
30.350	103.130	-150.720	30.350	103.110	-117.400
30.350	103.080	-7.520	30.370	103.070	-7.520
30.350	103.030	-114.400	30.340	103.030	34.400
30.350	103.010	-7.520	36.320	104.990	-108.220
30.350	104.730	-14.200	30.320	104.920	-114.800
30.330	104.240	123.400	30.300	104.240	142.000
30.320	104.430	104.100	35.700	104.470	173.500
30.700	104.490	-1.510	30.750	104.510	-174.000
30.720	104.530	-1.100	30.710	104.540	-1.010
30.890	104.570	51.610	30.670	104.600	177.000
30.800	104.630	-53.200	30.640	104.600	-7.000
30.830	104.730	103.580	35.600	104.740	57.000
30.800	104.750	11.510	30.600	104.770	132.000
30.800	104.730	19.280	30.560	104.750	114.400
30.800	104.750	126.230	30.540	104.810	155.300
30.500	104.850	-29.190	30.530	104.800	-54.100
30.520	104.890	-30.700	30.500	104.810	-30.500
30.570	104.940	-120.420	30.500	104.970	-1.500
30.590	104.970	-53.860	30.510	104.910	-31.400
30.530	103.040	-72.480	30.560	104.400	72.200
30.600	104.490	277.100	30.570	104.320	212.100
30.630	104.550	175.190	30.590	104.300	132.100
30.690	104.510	210.170	30.580	104.640	108.310
30.600	104.730	212.350	30.340	104.710	45.000
30.600	104.750	71.470	35.810	104.700	56.000
30.400	104.820	75.150	30.450	104.840	39.300
30.400	104.800	55.210	36.820	104.900	110.000
30.830	104.930	53.410	36.800	104.920	91.700
30.790	104.940	113.570	30.800	104.900	13.040
30.830	104.400	551.750	46.590	104.400	17.500
30.700	104.400	530.070	30.820	104.470	259.700
30.900	104.500	-80.130	30.950	104.400	203.000
30.750	104.470	94.700	30.700	104.470	312.100
30.780	104.490	224.100	37.230	104.500	254.000
31.100	104.500	130.000	37.070	104.520	345.410
31.110	104.530	109.410	37.130	104.530	214.220
31.100	104.540	-171.090	37.130	104.500	-40.510
31.140	104.540	-123.780	37.120	104.600	-153.310
31.130	104.770	-73.550	37.130	104.140	-69.400
31.110	104.770	-62.340	37.130	104.500	-111.300
31.130	104.830	-17.330	37.130	104.070	81.000
31.150	104.900	151.910	37.110	104.900	353.410
31.150	103.040	-74.700	37.130	103.000	424.000
31.190	103.050	135.770	37.210	104.070	94.000
31.200	104.730	13.200	37.220	104.700	40.310
31.210	104.750	-32.540	37.240	104.770	-56.420
31.250	104.810	52.570	37.220	104.790	16.400
31.200	104.500	-150.460	37.230	104.500	-147.700
31.270	104.500	-170.000	37.190	104.510	-150.300
31.310	104.530	-56.720	37.330	104.570	74.000
31.300	104.590	177.220	37.300	104.000	443.300
31.400	104.530	386.240	37.420	104.600	457.700
31.500	104.570	321.320	37.370	104.700	580.900
31.200	104.720	439.370	37.320	104.700	501.100
31.320	104.730	501.130	37.320	104.620	332.240
31.320	104.840	303.290	37.320	104.070	103.320
31.300	104.820	215.100	37.300	104.700	273.000
31.330	104.980	344.070	37.330	103.000	337.500
31.340	103.010	575.470	37.400	103.050	102.150
31.330	103.000	527.000	37.330	103.050	242.800
31.330	104.070	174.180	31.320	103.070	71.000
31.310	104.710	292.040	37.320	104.090	302.000
31.340	104.670	311.180	37.330	104.630	280.000
31.330	104.000	225.840	37.440	104.660	687.300
31.370	104.670	627.010	37.470	104.700	454.400
31.370	104.700	550.290	37.340	104.710	352.700
31.370	104.750	552.180	31.390	104.740	150.340

LA I	LA II	LA III	LA I	LA II	LA III
37.520	104.770	247.110	37.010	104.030	327.510
37.530	104.830	250.080	37.030	104.080	435.510
37.540	104.920	009.190	37.080	104.940	715.570
37.550	104.960	020.370	37.130	105.030	331.020
37.040	105.040	206.530	37.070	105.020	160.810
37.080	105.000	147.210	37.050	105.000	38.480
37.020	105.010	-37.070	37.210	105.030	-23.410
37.240	105.040	-30.020	37.240	105.030	-13.720
37.270	105.040	42.700	37.290	105.030	25.300
37.320	105.070	-17.710	37.300	105.100	14.470
37.360	105.100	37.730	37.410	105.030	35.810
37.420	105.150	-30.320	37.430	105.030	-104.280
37.480	105.020	-133.910	37.500	105.020	-23.050
37.520	105.010	40.370	37.540	104.970	22.150
37.540	104.990	184.500	37.540	105.030	35.590
37.540	105.070	01.230	37.550	105.100	30.240
37.560	105.130	35.100	37.520	105.030	60.770
37.580	104.810	135.430	37.570	104.830	294.630
37.540	104.830	222.930	37.520	104.890	254.810
37.510	104.870	197.390	37.450	104.870	30.400
37.460	104.900	04.390	37.510	104.710	103.020
37.440	104.720	337.340	37.130	104.770	30.300
37.170	104.790	31.900	37.190	104.810	27.420
37.220	104.830	-31.150	37.240	104.840	3.010
37.250	104.850	11.270	37.270	104.840	3.140
37.230	104.830	13.280	37.200	104.800	30.270
37.380	104.730	144.510	37.380	104.760	102.930
37.390	104.770	123.200	37.420	104.700	137.200
37.450	104.700	151.310	37.410	104.740	240.440
37.130	104.810	-102.790	37.100	104.830	-104.350
37.190	104.800	-47.790			



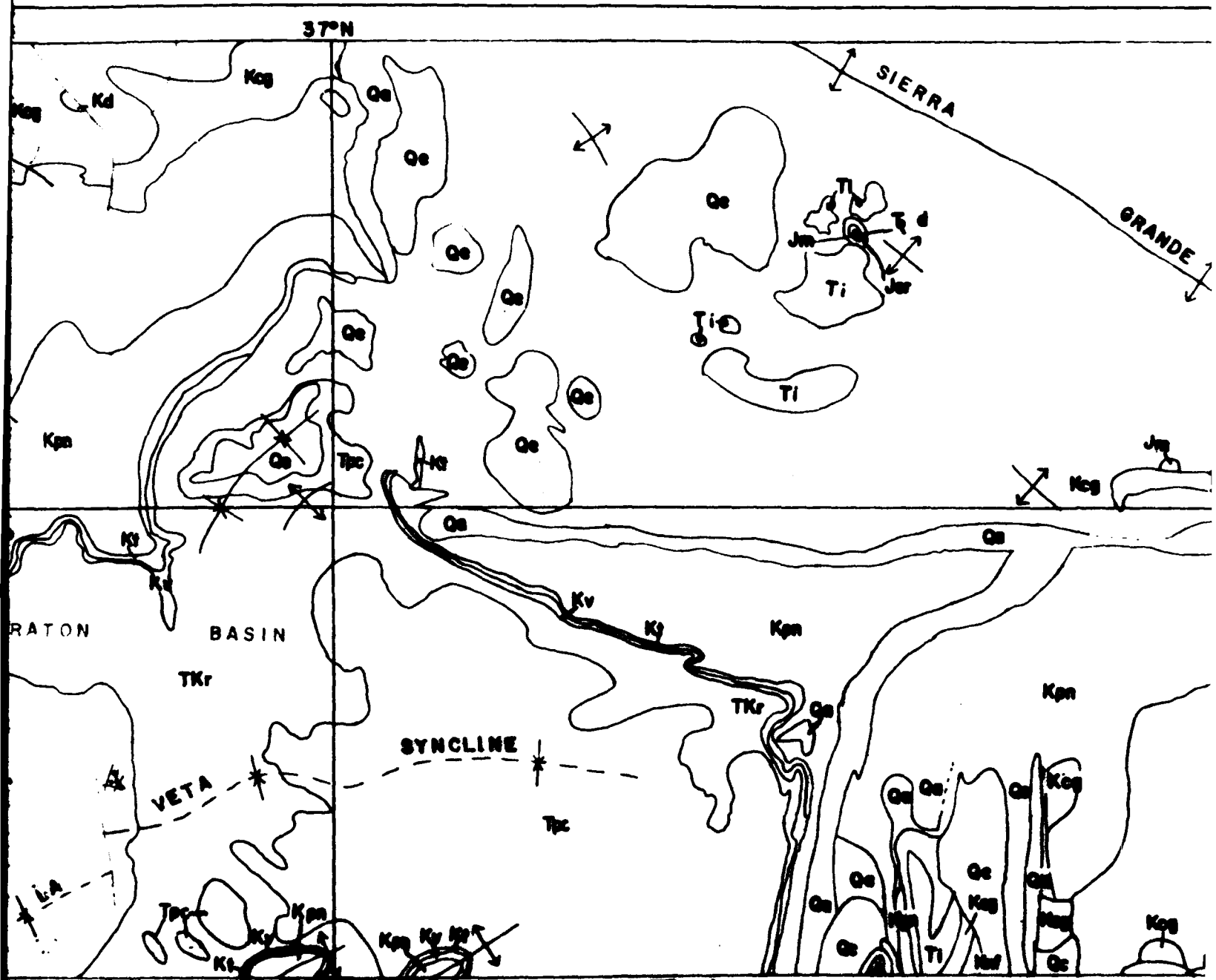
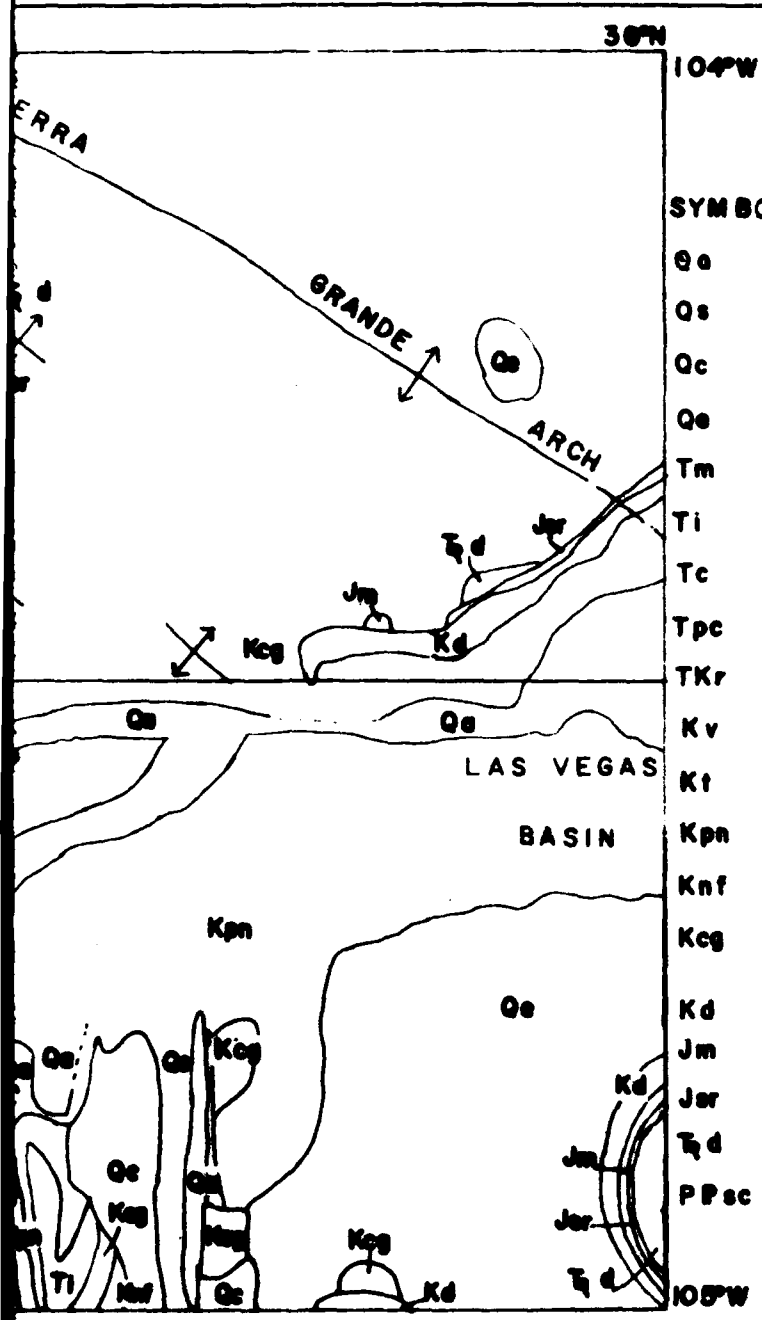


**PLATE I**  
**GEOLOGY AND STRUCTURE OF THE**  
**RATON BASIN OF N.M. AND COLO.**



LEGEND

SYMBOL FORMATION

- Qe alluvium
- Qs sand
- Qc landslide
- Qe volcanic rock
- Tm metamorphics
- Ti intrusives
- Tc Cuchera
- Tpc Poison Canyon
- TKr Raton
- Kv Vermejo
- Kt Trinidad
- Kpn Pierre
- Knf Niobrara
- Kcg Greenhorn  
Carlile  
Graneros
- Kd Dakota
- Jm Morrison
- Jer Entrada
- Tq d San Rafael
- PPsc Dockum Group
- Sangre de Cristo

FAULT (bell on downthrown side)

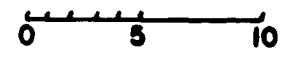
SYNCLINE

ANTICLINE

MONOCLINE

CONTACT

SCALE



NAUTICAL MILES

OF THE  
COLO.

38°N

ARCH  
0

APISHIPA  
0

UNNAMED

TROUGH

1500

0

-1500

-3000

DELCARBON SYNCLINE

SYNCL

WET MOUNTAINS

LA

VETA

RATON B.

9000

1800  
UNNAMED  
ANTICLINE

SPANISH PEAKS

BASE

RA'

37°N

3

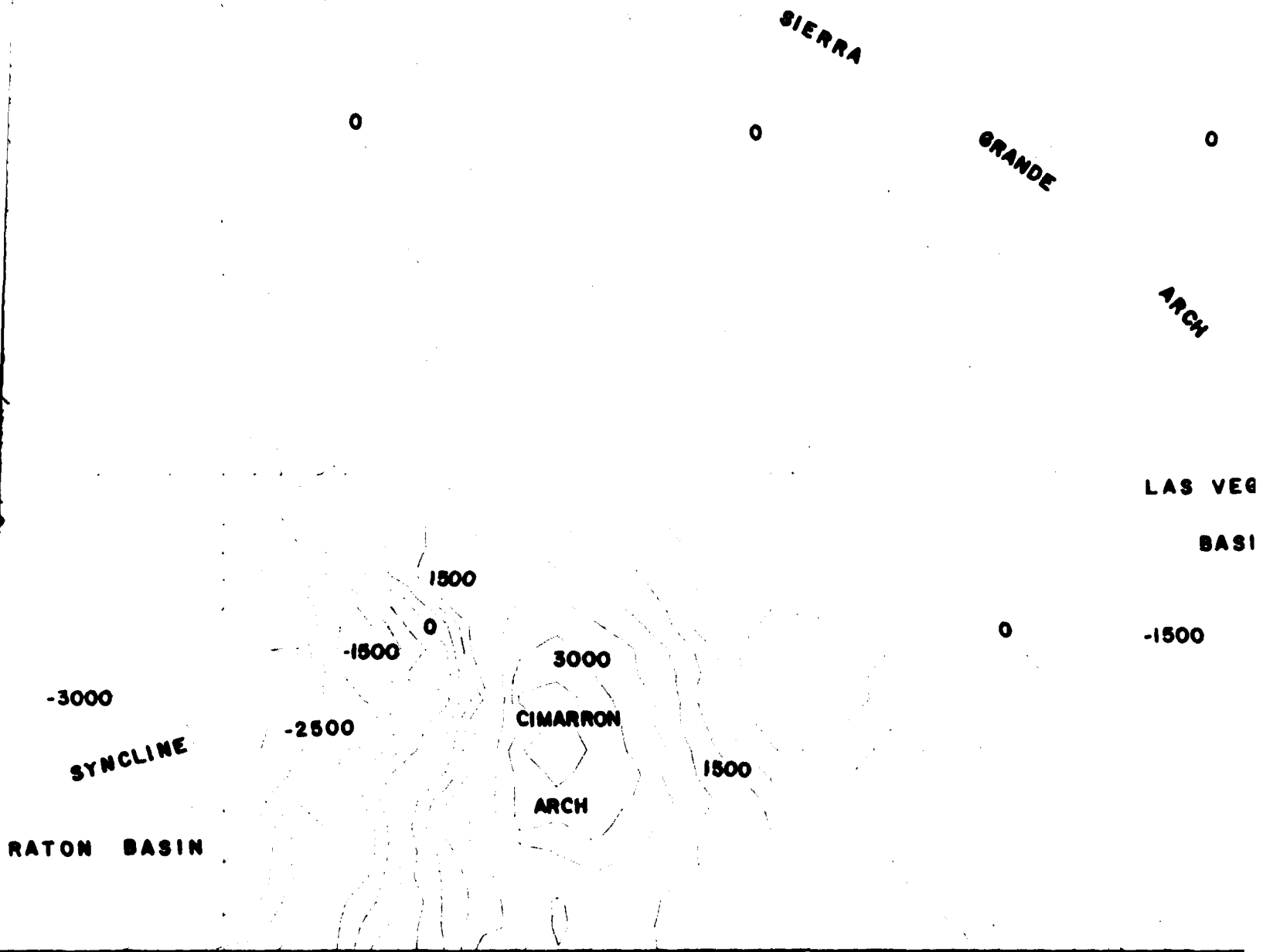


## PLATE 2

BASEMENT STRUCTURE MAP FOR THE  
RATON BASIN OF N.M. AND COLO.

36°N  
104°W

GRANDE

0

ARCH

LAS VEGAS  
BASIN

0

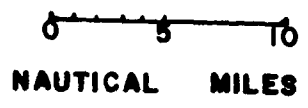
-1500

105°W

LEGEND

DATUM IS SEA LEVEL

SCALE



OR THE  
COLO.

37°45'N

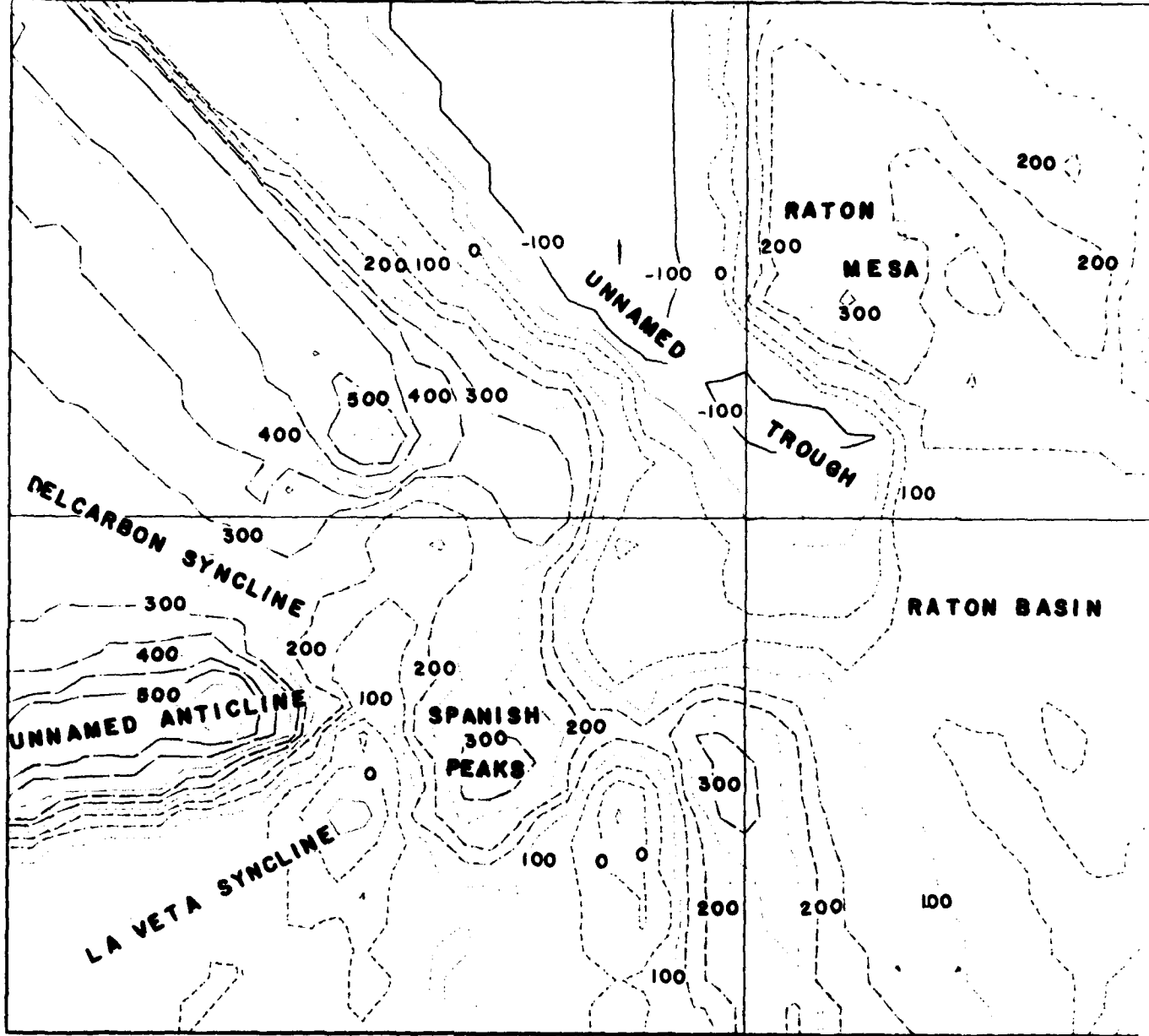


### PLATE 3

## GROUND MAGNETIC MAP RATON BASIN OF N.M. A

DATUM IS STATION ONE IN FIGURE

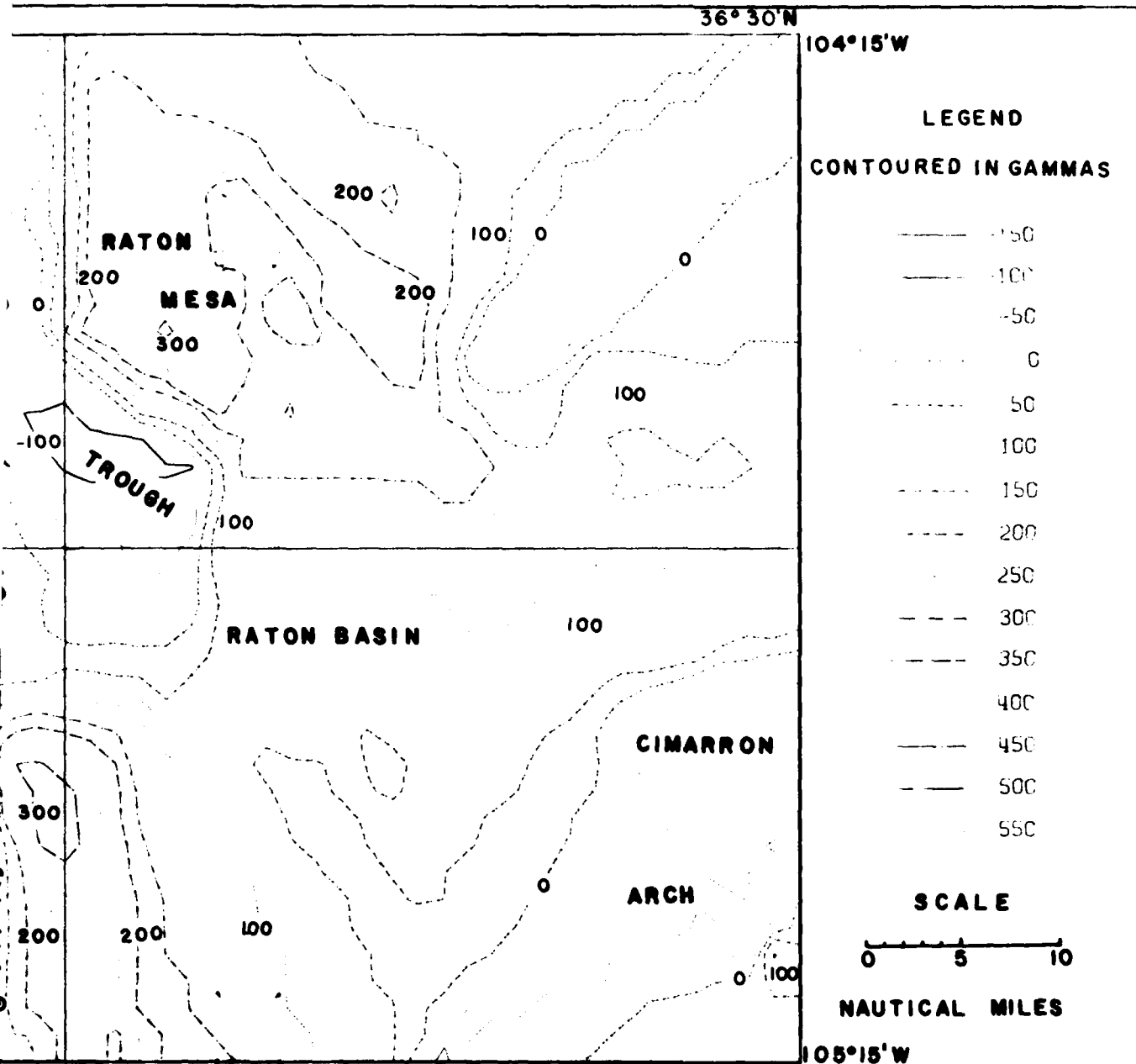


### PLATE 3

# MAGNETIC MAP FOR THE SIN OF N.M. AND COLO.

THIS IS STATION ONE IN FIGURE 14

DATE  
LMED  
8